National Library of Canada
Canadian Theses Service
Ottawa, Canada
K1A 0N4

Bibliothèque nationale du Canada
Services des thèses canadiennes

CANADIAN THESES

THÈSES CANADIENNES

NOTICE

The quality of this microfiche is heavily dependent upon the quality of the original thesis submitted for microfilming. Every effort has been made to ensure the highest quality of reproduction possible.

If pages are missing, contact the university which granted the degree.

Some pages may have indistinct print especially if the original pages were typed with a poor typewriter ribbon or if the university sent us an inferior photocopy.

Previously copyrighted materials (journal articles, published tests, etc.) are not filmed.

Reproduction in full or in part of this film is governed by the Canadian Copyright Act, R.S.C. 1970, c. C-30.

AVIS

La qualité de cette microfiche dépend grandement de la qualité de la thèse soumise au microfilmage. Nous avons tout fait pour assurer une qualité supérieure de reproduction.

S'il manque des pages, veuillez communiquer avec l'université qui a conféré le grade.

La qualité d'impression de certaines pages peut laisser à désirer, surtout si les pages originales ont été dactylographiées à l'aide d'un ruban usé ou si l'université nous a fait parvenir une photocopie de qualité inférieure.

Les documents qui font déjà l'objet d'un droit d'auteur (articles de revue, examens publiés, etc.) ne sont pas microfilmés.

La reproduction, même partielle, de ce microfilm est soumise à la Loi canadienne sur le droit d'auteur, SRC 1970, c. C-30.

THIS DISSERTATION
HAS BEEN MICROFILMED
EXACTLY AS RECEIVED

LA THÈSE A ÉTÉ
MICROFILMÉE TELLE QUE
NOUS L'AVONS REÇUE

NL-339 (r. 86/06)

Canada

THE UNIVERSITY OF ALBERTA

SEALED RADIO FREQUENCY-EXCITED CARBON DIOXIDE WAVEGUIDE LASERS

BY

© BRUCE A. MCARTHUR

A THESIS

SUBMITTED TO THE FACULTY OF GRADUATE STUDIES AND RESEARCH

IN PARTIAL FULFILMENT OF THE REQUIREMENTS FOR THE DEGREE

OF MASTER OF SCIENCE

DEPARTMENT OF ELECTRICAL ENGINEERING

EDMONTON, ALBERTA

FALL 1986

Permission has been granted to the National Library of Canada to microfilm this thesis and to lend or sell copies of the film.

The author (copyright owner) has reserved other publication rights, and neither the thesis nor extensive extracts from it may be printed or otherwise reproduced without his/her written permission.

L'autorisation a été accordée à la Bibliothèque nationale du Canada de microfilmer cette thèse et de prêter ou de vendre des exemplaires du film.

L'auteur (titulaire du droit d'auteur) se réserve les autres droits de publication; ni la thèse ni de longs extraits de celle-ci ne doivent être imprimés ou autrement reproduits sans son autorisation écrite.

ISBN 0-315-32391-4

THE UNIVERSITY OF ALBERTA

RELEASE FORM

NAME OF AUTHOR: Bruce A. McArthur

TITLE OF THESIS: Sealed Radio Frequency-Excited Carbon Dioxide Waveguide Lasers

DEGREE: Master of Science

YEAR THIS DEGREE GRANTED: 1986

Permission is hereby granted to THE UNIVERSITY OF ALBERTA LIBRARY to reproduce single copies of this thesis and to lend or sell such copies for private, scholarly or scientific research purposes only.

The author reserves other publication rights, and neither the thesis nor extensive extracts from it may be printed or otherwise reproduced without the author's written permission.

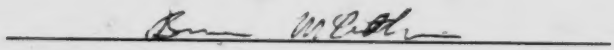

#207, 10655 83 Ave
EDMONTON, Ab
T6E 2E3

Date: Sept 2/86

THE UNIVERSITY OF ALBERTA

FACULTY OF GRADUATE STUDIES AND RESEARCH

The undersigned certify that they have read, and recommend to the Faculty of Graduate Studies and Research for acceptance, a thesis entitled SEALED RADIO FREQUENCY-EXCITED CARBON DIOXIDE WAVEGUIDE LASERS

submitted by BRUCE A. MCARTHUR

in partial fulfilment of the requirements for the degree of MASTER OF SCIENCE

(Supervisor)

Date: Sept 2/86

ABSTRACT

This thesis describes a study of the lifetime-limiting factors in sealed radio frequency-excited carbon dioxide waveguide lasers. Several significant goals were achieved as a result of this work. First, a set of procedures concerning the design and construction of sealed CO_2 lasers was established. Using these as guidelines, a 5 watt epoxy-sealed waveguide laser was constructed and two prototype metal-sealed lasers were designed. Secondly, a high-vacuum laser processing station equipped with a residual gas analyzer for the on-line sampling and analysis of laser gas mixtures was designed and constructed. A series of experiments were then carried out to determine the effects of pressure, gas mixture, input power, and residual gas contaminants on CO_2 dissociation and laser output power. The results of these studies both extend the range of previously published data on RF-excited CO_2 laser gas discharges and are of direct application to the development of surgical CO_2 laser systems at the Department of Electrical Engineering's Medical Laser Lab.

ACKNOWLEDGEMENTS

I would like to express my thanks to Dr. J. Tulip for his guidance and support over the past three years.

I wish also to thank G. Fij and H. Gans for their machining skills which were invaluable in the contruction of the laser structures and laser processing station.

Special mention also goes to K. Westra for his assistance in the calibration of the RGA and analysis of the gas chemistry data and to M. Paulson for the many brainstorming sessions concerning RF phenomena and laser design.

TABLE OF CONTENTS

CHAPTER	PAGE
1. INTRODUCTION	1
2. SEALED LASER DESIGN	8
2.1 Design Considerations	8
2.2 The 5 Watt Epoxy-Sealed Laser	17
2.3 Hard-Sealed Laser Design	22
3. DESIGN OF A LASER PROCESSING STATION FOR LIFETIME EXPERIMENTS	28
3.1 The Measurement of Laser Gas Composition	28
3.2 Gas Sampling Techniques	32
3.3 Laser Processing Station Design	37
3.4 Gas Analyzer Calibration	46
4. LASER GAS CHEMISTRY EXPERIMENTS	57
4.1 Experimental Procedures	57
4.2 Preliminary Measurements	60
4.3 CO_2 Dissociation Measurements	66
4.4 Hydrogen and Water Vapor Measurements	76
4.5 Optical Damage	83
5. CONCLUSIONS AND RECOMMENDATIONS	85
REFERENCES	89

LIST OF TABLES

Table	Description	Page
2-1	Outgassing Rates as a Function of Bake-Out Temperature	14
3-1	Ionization Efficiency of Laser Gases	47
3-2	Cracking Coefficients for N_2, CO, and CO_2	49
3-3	Calibration Coefficients for CO_2, N_2, CO, O_2, and H_2	56

LIST OF FIGURES

Figure	Description	Page
2-1	Two Basic CO_2 Waveguide Laser Designs	10
2-2	The 5 Watt Soft-Sealed Laser	18
2-3	Cross-section through the Soft-Sealed Laser Discharge Structure	19
2-4	Laser Output Power vs RF Input Power in the 15cm Soft-Sealed Laser	21
2-5	Cross-section through the Hard-Sealed Laser	24
2-6	Hard-Sealed Laser Waveguide Structure	25
3-1	Pump Configurations for Laser Gas Sampling	34
3-2	Gas Flows in Single Aperture Differential Pumping	35
3-3	The Laser Processing Station	40
3-4	Block Diagram of the Laser Processing Station	41
3-5	Residual Gas Analysis of the Laser Processing Station	45
3-6	Cracking Coefficients vs Pressure for N_2 and CO	50
3-7	Cracking Coefficients vs Pressure for CO_2	51
3-8	Mass Scan of a Representative Laser Gas Sample	53
3-9	Separation of Principal Peaks in a Laser Gas Sample	54
4-1	Measurements of the Diffusion Time Constant for CO_2 through a 3:1 He:N_2 Gas Mixture	59
4-2	Preliminary Lifetime Test - Laser Output Power and CO_2 Partial Pressure vs Time	61
4-3	Preliminary Lifetime Test - CO and O_2 Partial Pressure vs Time	62
4-4	Preliminary Lifetime Test - Water vapor and Hydrogen Pressure vs Time	64

LIST OF FIGURES (cont.)

Figure	Description	Page
4-5	CO_2 Partial Pressure vs Time as a Function of Pressure	68
4-6	CO_2 Dissociation vs Pressure^{-1}	69
4-7	CO_2 Partial Pressure vs Time as a Function of He Content	70
4-8	CO_2 Partial Pressure vs Time as a Function of Xe Content	71
4-9	CO_2 Partial Pressure vs Time as a Function of RF Input Power	73
4-10	O_2 Partial Pressure vs Time as a Function of RF Input Power	74
4-11	H_2O Partial Pressure vs Time as a Function of RF Input Power	75
4-12	Water Vapor Test - Laser Output Power and Water Vapor Concentration vs Time	78
4-13	Laser Output Power vs Water Vapor Concentration	79
4-14	Hydrogen Test - Laser Output Power and Hydrogen and Water Vapor Concentrations vs Time	80
4-15	Laser Output Power vs Hydrogen Concentration	81
4-16	CO_2 and O_2 Partial Pressures as a Function of Hydrogen and Water Vapor Content	82

LIST OF SYMBOLS

Symbol	Definition
RF	radio frequency
DC	direct current
e	electron
v_d	electron drift velocity
d	electrode separation
λ	electrical wavelength
t	time
Q	gas flow rate
C	conductance
p	pressure
S	pumping speed
V	volume

CHAPTER 1
INTRODUCTION

The compact CO_2 waveguide laser, having a continuous output power of between 2 and 50 watts, has become increasingly popular for low-power medical, industrial, and military applications over the past decade because of its rugged construction and long sealed lifetime. For surgical applications, waveguide laser technology is an ideal replacement for the conventional flowing-gas CO_2 laser, which requires fragile glass tubes, bulky vacuum pumps and gas bottles. A surgical CO_2 laser system, based on a metal-sealed radio frequency-excited CO_2 waveguide laser with an output power of at least 50 watts, is currently under development at the Medical Laser Lab at the University of Alberta. The goal of this project is to study the lifetime-limiting factors in sealed radio frequency-excited CO_2 waveguide lasers in order to produce a sealed high-power laser with an operating lifetime of 1000 hours.

Waveguide lasers were first operated using high-voltage DC excitation. Reports of sealed-off operation were made as early as 1973 by Abrams and Bridges[1], although it was not until 1976 that the first studies of extended lifetime were made by Hochuli[2] and Laughmann[3]. Hochuli extended his earlier work on cathode materials in sealed conventional CO_2 lasers[4] to a study of discharge tubes with the dimensions (0.6 to 1.0 mm diameter) and pressures (100 to 200 torr) found in waveguide lasers. Results indicated 5000 hour lifetimes could be expected although his initial tests with laser tubes were disappointing. Laughmann obtained 2600 hour operation from an epoxy-sealed DC-excited laser with a beryllium oxide waveguide and copper electrodes.

In 1977, the use of radio-frequency excitation, applied transversely to the waveguide structure, was reported[5,6]. Subsequent studies demonstrated that RF excitation has a number of advantages over DC excitation. The RF discharge has a positive impedance characteristic which results in greater stability and allows the elimination of ballast resistors thus providing increased efficiency. The lower discharge voltage of the RF discharge also allows a more optimal excitation of CO_2 gas molecules. As a result, lasers with both high efficiencies (13%)[7] and very high output powers per unit length (> 0.8 W/cm)[7] have been produced. Furthermore RF-excited lasers can be scaled to higher output powers more easily because the transverse discharge scales by current rather than by voltage as is the case for longitudinally excited DC discharges. The RF discharge also can be directly modulated thus eliminating any requirement for external shutters in pulsed operation. Most significantly, for the purposes of this investigation, it has been claimed that RF excitation results in significant increases in sealed lifetime. The first reports of sealed lifetime from a RF-excited CO_2 waveguide laser were made by Laakmann[8] who reported 3000 hour lifetimes .

DC-excited CO_2 lasers exhibit a number of plasma chemical processes which limit sealed lifetime. The most important of these are the dissociation of CO_2 and cathode sputtering. The dissociation of CO_2 is caused primarily by impact with 7eV electrons[9] (the reaction has a cross-section which peaks strongly at 6.9eV) as described by the equation

$$e + CO_2 \rightarrow CO_2^* + e \rightarrow CO + O + e$$

(the asterisk denotes CO_2 in a highly excited state). Other less important dissociation mechanisms include dissociative attachment[10]

$$e + CO_2 \rightarrow (CO_2^-)^* \rightarrow CO + O^-$$

and molecular collisional dissociation[10]

$$M^* + CO_2 \rightarrow CO_2^* + M$$

$$CO_2^* \rightarrow CO + O$$

(M is another molecule present in the discharge).

In the DC discharge, a large positive space charge is formed adjacent to the cathode. The high electric fields resulting from this positive space charge cause sufficient numbers of 7 eV electrons to be emitted by the cathode to cause a high degree of dissociation in the laser gas mixture. Dissociation levels of 70 to 90% in conventional DC-excited CO_2 lasers are quite common.

Equilibrium dissociation levels are largely determined by the reformation of CO_2 through the reaction[11]

$$CO + OH \rightarrow CO_2 + H.$$

This has been substantiated by mass spectroscopic analysis of the laser gas mixture by Witteman and Werner[13], and Smith[14]. Hydroxyl ions are formed by the dissociation of outgassed water vapor or from a reaction between outgassed hydrogen and the oxygen resulting from CO_2 dissociation. As a result, hydrogen has been widely used as an additive in sealed DC-excited CO_2 laser gas mixtures[12]. Smith and Browne[15] demonstrated that the addition of 0.1 to 0.5 torr of hydrogen to a low pressure discharge reduced CO_2 dissociation levels from 87% to 40%. Other catalytic agents, most notably platinum[16,17], have also been found to reduce the level of CO_2 dissociation. Nonetheless, over longer periods of time, oxygen is absorbed by tube and electrode surfaces, shifting the chemical equilibrium towards greater dissociation, until eventually the CO_2 is consumed and laser oscillation ceases.

Cathode sputtering results when positive ions, attracted by the high electric fields across the cathode dark space, impact the surface of the cathode and cause the ejection of metal ions. This results in the deposition of thin films in the cathode region. If thin film deposition occurs on the optics, the reflectivity will be changed and thus directly affect laser output power. Metal films deposited in the laser bore can react with gas components and thus contribute to gas deterioration. Cathode material can also be transported over far greater distances than by sputtering alone if gaseous complexes involving cathode materials are formed. These complexes are transported by diffusion and break up on collision with laser tube surfaces. Cathode effects are accentuated in the DC-excited waveguide laser[18] relative to a conventional DC-excited CO_2 laser because of the small dimensions of the waveguide (1.5-2.5mm diameter vs 20mm diameter), smaller numbers of gas molecules (10-100 times less), and higher discharge currents (up to 10 times higher). Much of the recent work in DC waveguide laser design has concentrated on the development of stable sputter-free cathode materials[19].

The primary lifetime advantage of the RF discharge is that neither the cathode nor the cathode fall region found in DC discharges are present; thus, electrode sputtering has been reported to be negligible[20]. The RF discharge is operated in the diffusion regime[21], in which neither electrons nor ions are able to traverse the electrode gap during a half-cycle of the applied electric field. The excitation frequency must then exceed v_d/d, where d is the electrode separation and v_d is the electron drift velocity . For a typical 2 mm waveguide, this results in a minimum excitation frequency of about 30 MHz. Above this frequency, electrode interactions are limited to the diffusion of electrons and ions to the walls. In order to further reduce the possibility of sputtering, electrodes in fact

can be made completely external to the discharge and capacitively coupled through the waveguide walls. Relatively few studies have been made of CO_2 dissociation in RF discharges. However, dissociation levels of up to 90%, comparable to levels in DC-excited discharges, have been reported[22]. As in the DC-excited lasers, equilibrium dissociation levels appear to be determined by reactions with water vapor. Limits to sealed lifetime in RF-excited waveguide lasers can be traced to one of two factors: degradation of the laser gas mixture or optical damage[23]. Reports of gas degradation have dealt primarily with the effects of water vapor on sealed lasers and the long term absorption of oxygen on laser tube surfaces.

The direct effects of hydrogen and water vapor on the excitation of CO_2 have been widely investigated. In initial tests, Witteman[12] claimed a factor of two increase in output power with the addition of water vapor and credited this to increased relaxation of the 01^10 laser level. Deutsch and Harrigan[24] subsequently claimed that power increases attributed to water vapor were in fact caused by its effect on CO_2 dissociation. Cheo and Cooper[25] demonstrated that if an optimal CO_2 pressure was maintained, gain decreases monotonically with increasing H_2O and H_2 gas pressure. Measurements[26] of vibrational relaxation rates in CO_2 laser gas mixtures revealed that H_2O and H_2 both severely relax the 00^01 laser level (with relaxation rates of 4.2×10^4 torr^{-1} s^{-1} and 4.5×10^3 torr^{-1} s^{-1} respectively). Water vapor was also found to produce a bottleneck at the 01^10 level through a process such as

$$H_2O(010) + CO_2(00^00) \rightarrow H_2O(000) + CO_2(10^00) + 207\ cm^{-1}.$$

Later work by Smith and Austin[9] showed that the beneficial effect of hydrogen as a result of CO_2 reformation could be observed at partial pressures of up to 0.2 torr. The decreases in output power observed at higher hydrogen partial

pressures were however attributed to a modification of the electron energy distribution away from the optimum value for excitation of the 00^01 laser level rather than to vibrational relaxation. Browne and Smith[17] also demonstrated that if an alternative means of controlling CO_2 dissociation is used (such as a distributed platinum catalyst), hydrogen in any amount will decrease laser output power.

The deleterious effects of water vapor appear to be enhanced in the sealed waveguide laser. Pace and Cruickshank[27] reported a correlation between the partial pressure of water vapor and a decrease in laser power output in experiments with sealed DC-excited waveguide lasers. Water vapor concentrations as low as 0.1 to 0.5% were found to inhibit laser action. Although outgassing could not be eliminated by vacuum baking, Pace and Cruickshank obtained lifetimes in excess of 5000 hours from epoxy-sealed laser tubes using a P_2O_5 getter to absorb water vapor. Laakmann has also stated that hydrogen and water vapor outgassing is a primary cause of gas degradation in RF-excited lasers[23]. Their solutions to this problem include a palladium getter to absorb outgassed hydrogen and a cellulose getter to absorb water vapor[28].

The specific goals of this study have been to provide a body of knowledge for the design of sealed CO_2 waveguide lasers and, in doing so, examine a number of the plasma chemical processes in RF-excited CO_2 discharges which have not been investigated adequately in the literature. Chapter 2 discusses important factors involved in the design of a sealed laser including materials, sealing techniques, and laser tube processing. These studies were then used as guidelines for the construction of an epoxy-sealed 5 watt laser and the design of two prototype metal-sealed lasers. Chapter 3

examines some alternative measurement techniques which can be used for gas analysis in sealed CO_2 lasers. The design, construction, and calibration of a high-vacuum laser processing station equipped with a residual gas analyzer is then discussed. Chapter 4 describes a number of experiments which were carried out to determine the effects of pressure, gas mixture, input power, as well as hydrogen and water vapor on CO_2 dissociation and laser output power.

CHAPTER 2
SEALED LASER DESIGN

The demand for CO_2 laser systems which are portable, reliable, and affordable makes the sealed laser, with its freedom from vacuum pumps and gas bottles, a virtual necessity. This chapter considers the factors involved in the design of sealed CO_2 waveguide lasers including materials, sealing techniques, and laser tube processing. A 5 watt epoxy-sealed laser, used in the gas chemistry experiments of Chapter 4, and the design for two prototype metal-sealed lasers are then presented.

2.1 Design Considerations

The basic design for an RF-excited CO_2 waveguide laser has been discussed extensively in the literature (see for example the overview presented by Sinclair[29]) and thus will be presented here only in summary form. The waveguide laser differs from a conventional CO_2 laser in that the hollow waveguide both contains the discharge and guides the light inside the laser cavity. It is crucial that the waveguide material have a high thermal conductivity to allow the efficient cooling of the laser gas mixture. The waveguide laser must also be fabricated with minimum distributed losses, ie. optical absorption (waveguiding) losses, optical scattering losses, waveguide bending losses, and coupling losses between the waveguide and laser mirrors. Transverse mode stability is enhanced if the waveguide is of homogeneous construction with symmetrical cooling. Ceramic waveguides, fabricated from alumina, beryllia, and boron nitride, have all been used successfully in laser designs. Alumina, although inferior to beryllia in both thermal conductivity and optical absorption, is the most widely used waveguide material because it is safe (beryllia dust is

toxic), strong, and can be polished to an excellent surface finish. Coupling losses can be restricted to less than 0.3% per mirror by placing the optics 2 mm or less from the ends of the waveguide.

The homogeneous deposition of RF input power throughout the gas volume inside the waveguide is an equally important design consideration. The discharge structure, which can be viewed as a lossy transmission line, will have significant(> 10%) longitudinal voltage variations if its length exceeds 7% of its electrical wavelength[30,31]. Inductors, placed at periodic locations along the length of the waveguide, have been used to reduce voltage variations to less than 5%. Griffith[31] obtained a 130% increase in output power using this technique on a laser with a length of 0.67λ.

Two basic designs have evolved in the construction of sealed CO_2 wave - guide lasers. The first, especially popular for DC-excited waveguide lasers, uses the waveguide as a vacuum enclosure. As shown in Figure 2-1a optical mounts are attached directly to the ends of the waveguide. In the second design, shown in Figure 2-1b, the waveguide is placed inside a sealed metal or glass enclosure. This allows the natural incorporation of gas ballast volume and eliminates the problem of sealing the ceramic.

The requirement for long-term sealed operation restricts the choice of materials and sealing techniques to those which are compatible with accepted high-vacuum technology. As explained in Chapter 1, limits to sealed lifetime can in general be traced to degradation of the laser gas mixture or optical damage. Gas degradation can be divided into the two following subareas:

Figure 2-1

Two basic CO_2 Waveguide Laser Designs

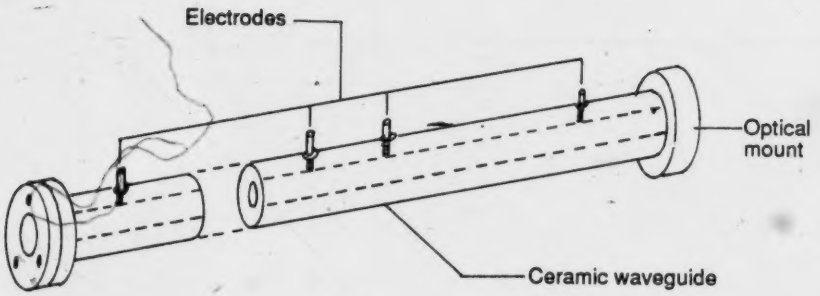

(a) Ceramic Tube Laser (DC-excited)

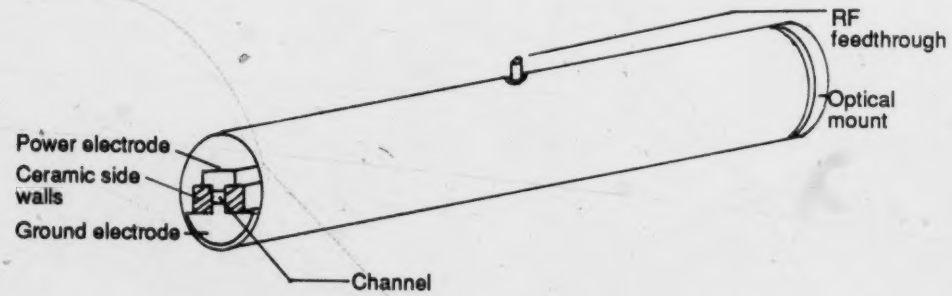

(b) Metal Tube Laser (RF-excited)

(1) Passive changes in gas composition caused by leaks in the vacuum enclosure and the outgassing of residual contaminants from surfaces internal to the laser.

(2) Changes in gas composition caused by chemical reactions between discharge products.

These two areas can also be interrelated as is the case for water vapor, released by outgassing, which catalyzes the reformation of CO_2 in the RF discharge.

Passive factors largely determine the shelf-life of a sealed laser. Leak rates can be reduced to negligible levels ($< 10^{-10}$ torr-l/s) by using high-vacuum sealing techniques but the seals must be sufficiently rugged to allow reliable leak-free operation of the laser in a wide range of operating conditions. Leak rates remain essentially constant, assuming no damage occurs to the vacuum envelope, whether or not the laser is operating.

The choice of sealing technology is determined largely by whether the laser design uses a metal or ceramic vacuum enclosure. Virtually all commercial waveguide laser manufacturers have rejected soft seals (O-rings or epoxies) for hard-sealing technologies (metal-to-metal, metal-to-ceramic, and ceramic-to-ceramic seals) which provide the reliability required for long-term operation[28]. Metallization and vacuum or hydrogen brazing have been widely used for the ceramic-to-ceramic and ceramic-to-metal seals in ceramic tube lasers[19,32]. This is a proven technology, used extensively for feedthroughs in high-vacuum systems and electronic tubes, which results in strong, reliable seals[35]. Ceramic-to-ceramic seals have also been successfully fabricated using a borosilicate glass suspension which is spray-coated onto ceramic parts and fired to produce

a permanent fused seal[33]. Optical contact thermo-diffusion bonding has been used for joining ceramic parts[33]. In this technique polycrystalline alumina surfaces which are polished flat and optically contacted are bonded together at a temperature 600°C below their melting point. Inert-gas welding, a standard technique for high-vacuum system construction, can be used for the sealing of lasers which use an external metal (preferably stainless steel) vacuum enclosure. It has been rejected by some manufacturers however because it results in excessive thermal stress to laser components[28]. Alternatively, a number of advanced beam-welding technologies, such as electron-beam welding at Hughes Aircraft[34] and CO_2 laser welding at Ferranti[19], have been applied to the fabrication of metal-to-metal seals. Beam welding causes only localized heating which allows welds to be placed close to temperature-sensitive components such as optics, and also allows a size reduction in the assembled device. Hard seals have also been applied to optics, where the most extensively used technique is indium soft-solder seals[33].

Outgassing occurs as a result of a number of different processes, the most important of which are surface desorption and diffusion. All laser tube parts which have been exposed to the atmosphere will have layers of adsorbed gas molecules, chiefly water vapor, on their surfaces and contain absorbed atoms of gas which have diffused inside them. Much of this gas load will be removed during pump-down as the trapped gases diffuse to the surfaces and weakly bound surface layers are stripped away. Outgassing rates decrease with time (desorption has a time constant of t^{-1} and diffusion has a time constant of $t^{-1/2}$)[36] and increase with temperature. The standard technique for reducing outgassing is thus to bake parts under vacuum at high temperature for extended periods of time. The processing procedure for laser tube parts used by

Laakmann Lasers includes a 100°C vacuum prebake for at least 72 hours, immediate assembly, followed by another 100°C bakeout of the assembled laser with the optics installed[28].

Candidate laser tube materials should thus be nonpermeable and capable of withstanding the vacuum bakeout necessary to reduce outgassing rates.Three standard high-vacuum materials: stainless steel, aluminum, and ceramic can be used to fabricate virtually all laser parts with the exception of optics.Outgassing rates for these materials as a function of bakeout temperature is shown in Table 2-1.

It is possible to estimate the leak and outgassing rates which are consistent with a six month shelf-life. The maximum allowed contamination level over a six month (4400 hour) period will be set at 1.0%. This is rather high but not unreasonable as the major atmospheric gas components (nitrogen, oxygen, and carbon dioxide) are already present in the laser gas mixture. Assuming a gas pressure of 120 torr and a gas volume of 100 cm^3 the maximum allowed leak rate would be 7.6×10^{-9} torr l/s. This requirement could be met with any of the high-vacuum sealing techniques discussed previously.

In a similar fashion it is possible to estimate the maximum allowed outgassing rate for adsorbed gases from the internal surfaces of the laser tube. Only water vapor and hydrogen will be considered as they are the most widely acknowledged contaminants of CO_2 waveguide lasers. Assuming a maximum contamination level of 0.1% the resulting outgassing rate is 7.6×10^{-10} torr l/s. A laser tube with a length of 15 cm and a diameter of 4 cm would have an internal suface area of at least 400 cm^2 (making an allowance for the surface areas of internal laser tube parts). This would result in a surface outgassing

Table 2-1

Outgassing Rates as a Function of Bake-Out Temperature

Material and Preparation	Outgassing Rate (torr-l cm^{-2} s^{-1})	Ref.
Stainless steel		
- unbaked, 10hr pump-down	1.35×10^{-9}	37
- unbaked, electropolished, 10 hr pump-down	4.28×10^{-10}	37
- 30 hr bake-out at 250°C	3.0×10^{-12}	38
- 2 hr vacuum bake-out at 800°C	2.0×10^{-13}	39
- 3 hr vacuum bake-out at 1000°C	1.58×10^{-14}	40
Aluminum		
- unbaked, 10 hr pump-down	6.0×10^{-10}	37
- 15 hr vacuum bake-out at 250°C	4.0×10^{-13}	38
Alumina		
- unbaked, 20 hr pump-down	8.25×10^{-8}	41

rate of 1.9×10^{-12} torr l/(cm^2 s).As shown in Table 2-1 a bakeout in excess of 250°C would be required to reduce outgassing levels to meet this requirement.

Processing temperatures for assembled lasers are limited to approximately 100°C by the temperature-sensitive nature of the dielectric coatings on the laser optics[28]. It is very difficult to achieve the necessary outgassing rates for hydrogen and water vapor by baking alone. As a result, designers of sealed CO_2 waveguide lasers have turned to a number of materials, called getters, which adsorb hydrogen and water vapor. The main requirement for these materials is that they possess a high sorptivity for hydrogen and/or water vapor without adsorbing or reacting with the other gases in the laser. An additional requirement is that the getter has a sorptivity which decreases with increasing temperature so that any previously adsorbed hydrogen and/or water vapor is evolved during bake-out. Phosphorus pentoxide (P_2O_5) removes water vapor by combining with it chemically to form phosphoric acid[42]. Pace and Cruickshank[27] reported 3000 hour lifetimes in sealed DC-excited waveguide lasers using a P_2O_5 getter. Cellulose compounds,when first baked under vacuum, have a large capacity for adsorbing water vapor. Cellulose cotton has been shown to have an adsorptivity of 0.12 mg/g at a water vapor pressure of 1μ at 20°C[43]. Cellulose getters were first used in CO_2 waveguide lasers by Laakmann[28]. Molecular sieves, synthetic aluminosilicate substances with a large capacity for water vapor, are not suitable because they have been found to adsorb oxygen as well as water vapor[27,28]. The most widely recognized hydrogen getters are the group B metals (Ti, V, Zr, Cb, La, Ce, Ta, Th, and Pd), which have a high hydrogen solubility that decreases with increasing temperature[42]. Palladium is preferred for lasers because its sorptivity for hydrogen decreases markedly from

60 cm^3/gm to 3.3 cm^3/gm between 20°C and 300°C. Palladium has previously been used as a means of controlling the hydrogen pressure in sealed conventional CO_2 lasers[16]. The first reported use of palladium in a sealed waveguide laser was made by Laakmann[28]. Powdered palladium was prepared by baking at 150°C in a vacuum of at least 10^{-4} torr for 12 hours.

The most important discharge-related effects are the loss of CO_2 caused by dissociation and the absorption of laser gases by laser tube surfaces. No materials commonly used for the construction of sealed CO_2 lasers have been reported to increase CO_2 dissociation. As discussed in Chapter 1, platinum has been reported to catalyze the reformation of CO_2 and can thus be of direct benefit to laser operation. The absorption of laser gases is primarily a problem in DC-excited lasers where cathode sputttering results in the deposition of reactive metal films. Reports of electrode sputtering in RF-excited lasers have been negative to date. A related problem which is present in RF-excited lasers is the absorption of the oxygen released by dissociation. It is thus important to choose tube materials which have stable surface oxides. Stainless steels are an excellent choice in this regard[36]. Processing techniques have also been successful in enhancing oxide stability. Laakmann use a nitric acid processing step to passivate nickel coatings used in the their lasers[28]. Laughmann[3] conditioned beryllia laser tubes with an oxygen discharge before beginning lifetime experiments.

Optical damage is a significant problem in sealed waveguide lasers primarily because the high power densities on the optics, on the order of 10kW/cm^2, make them extremely sensitive to particulate contamination or thin film deposition[23]. If particulate matter left in the laser tube lands on an optic it will burn a hole in the dielectric coating. The best defence against optical

damage is careful cleaning and assembly of the laser tube in a dust-free environment.

2.2 The 5 Watt Epoxy-Sealed Laser

Although hard-sealing is a necessity for reliable long-term laser lifetime an epoxy-sealed laser was felt to be more effective for short-term (less than 100 hours duration) measurements of the plasma chemistry inside sealed waveguide lasers. The primary concern was to meet high-vacuum construction standards with sealing techniques (epoxy, metal gaskets, and soft solder) which did not require extensive development work. As a high-power laser was not required for gas chemistry measurements and would have required a more complicated design, a compact 5 watt laser was constructed.

The assembled laser, shown in Figure 2-2, was built around a 15 cm long all- ceramic discharge tube with an external 100 cm^3 gas ballast tank. The waveguide structure, shown in cross-section in Figure 2-3, was constructed from two pieces of 94% alumina ceramic. Seals between the top and bottom plates, optical flanges, and the gas ballast were made using high-vacuum Torr-Seal epoxy.Soft-solder was used to seal metal parts on the optical flanges and ballast tank. An all ceramic structure with external electrodes was chosen for its enhanced mode stability and freedom from electrode sputtering. Also a hybrid metal/ceramic structure would have required four seals between dissimilar materials which was considered too unreliable. The 2.25 mm square waveguide was formed by cutting a groove in the bottom ceramic plate. The surfaces were then polished with a diamond grinding wheel.

Electrodes were capacitively coupled through the 1 mm thick waveguide walls. In addition to increasing discharge stability the external

Figure 2-2

The 5 Watt Soft-Sealed Laser

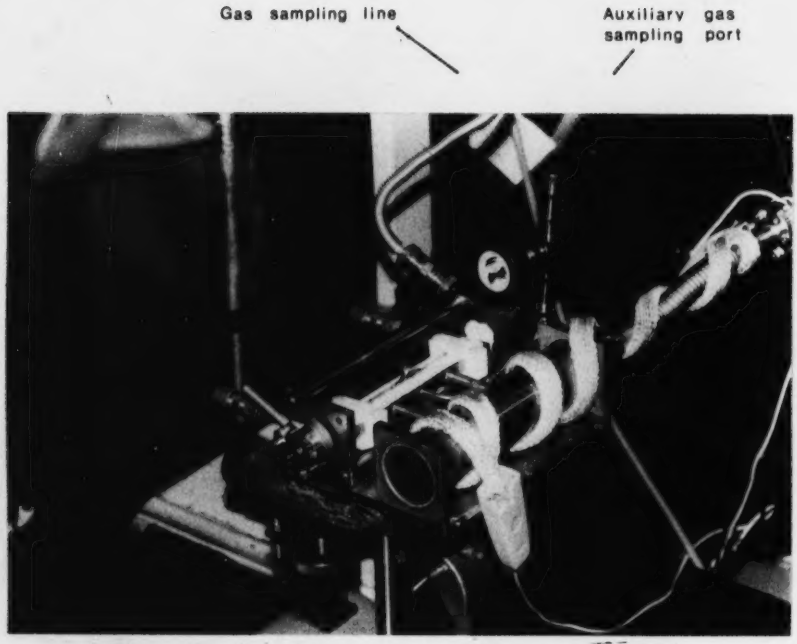

Figure 2-3

Cross-section through Soft-Sealed Laser Discharge Structure

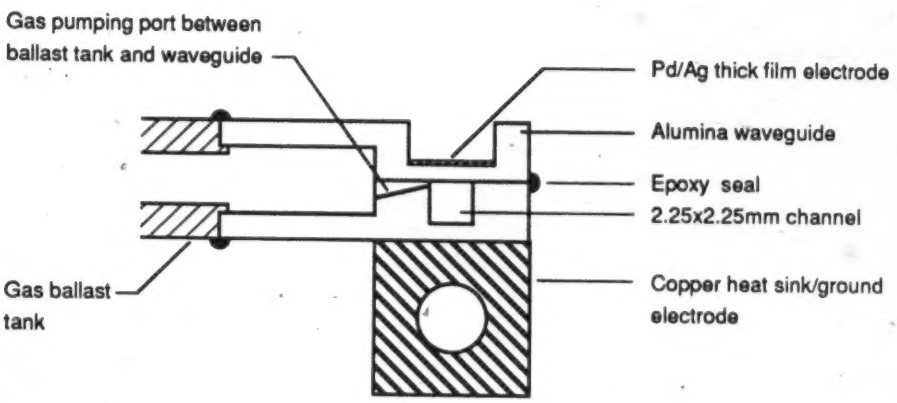

electrodes also eliminated the possibility of extraneous breakdown.The top electrode was fabricated using a metallized Pd/Ag thick film and the ground electrode was a hollow copper block, clamped to the waveguide structure, through which tap water was flowed for cooling. Gas flow between the waveguide and external gas ballast was permitted by three 0.5 mm by 1.0 mm channels. These were placed at the corner of the waveguide to minimize any optical losses. Gas sampling was possible from two locations: one on the back optical mount, the other at the entrance to the gas flow ports.

The optical end flanges and gas ballast tank were constructed from stainless steel. Optics were mounted approximately 2 mm from the ends of the waveguide on removable flanges which could be sealed with either viton O-rings or copper gaskets. An independent 1/4" diameter ZnSe output window was used to allow easy removal of the output coupler. The window was sealed by a crushed lead gasket. Optical alignments were made using a three-point adjustment scheme with a flexible bellows.

All laser tube parts were ultrasonically cleaned in separate baths of acetone, methanol, and distilled water. Ceramics were then prebaked at 1000°C. Final assembly was performed in a Class 100 laminar flow hood to minimize particulate contamination of the waveguide which could later result in damage to the optics. The assembled laser was leak tested and baked while under vacuum at 70°C for 72 hours. No evidence of contamination caused by epoxy, solder, or solder fluxes was detectable.

The laser was powered by a single 100 watt amplifier operating at 72 MHz. Connection from the amplifier to the laser was made through a 50Ω cable to a π matching network. A power connection was made to the center of

Figure 2-4

Laser Output Power vs RF Input Power
in the 15cm Soft-Sealed Laser

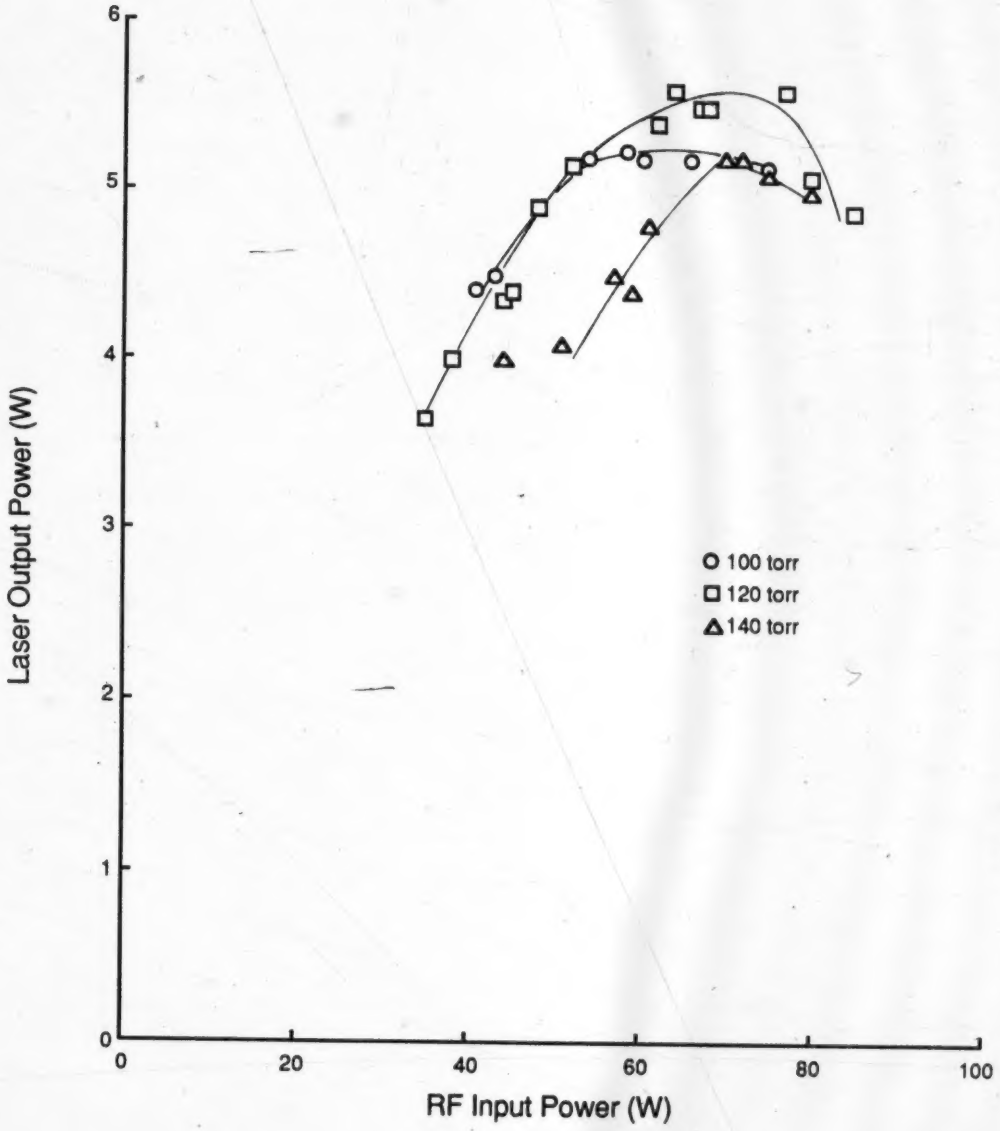

the top electrode on the laser. A parallel inductor, also connected at this point, was used to resonate the discharge structure at 72 MHz. Forward and reflected input power was monitored using a pair of Bird wattmeters.

The lasers operating characteristics were dominated by its low gain behavior, caused by the structures short length. It was necessary to increase the reflectivity of the output coupler to 95% in order to achieve laser oscillation. Nevertheless a maximum single-mode output power of 5.5 watts (0.37 W/cm) was obtained using a gas mixture of 12% CO_2, 12% N_2, 71% He, and 5% Xe at a pressure of 120 torr. Maximum efficiency was 11%. Output power versus input power at three pressures are shown in Figure 2-4. Output power was reduced in richer mixtures and ceased altogether at pressures above 140 torr. This is typical of low gain operation because rich mixtures have gain curves which drop off significantly at higher pressures. After a one-half hour warm-up period the laser showed very good mode stability and single-mode operation could be maintained over extended periods of time with only minor optical adjustments.

2.3 Hard-Sealed Laser Design

The prototype hard-sealed lasers are adaptations of a 60 cm O-ring-sealed laser under development by Murray Paulson[44]. Two versions of this laser were designed. The first will be sealed using a combination of tungsten-inert-gas welding and soft soldering in order to provide immediate feedback on the viability of the basic structure. In the second laser, soft soldering will be replaced by vacuum brazed seals. That however first requires extensive tests in order to produce high quality seals. The two lasers will then allow a side by

side comparison of the lifetime implications of soft soldering versus vacuum brazing.

The hard-sealed lasers have a number of significant design improvements over the soft-sealed laser. The lasers are much more compact, being completely contained (except for the vacuum pumping port) in a 3.8 cm diameter, 22.9 cm long stainless steel tube with 50% of the internal volume (300 cm^3) available for gas ballast. The discharge structure is designed to allow efficient cooling of the laser with an external heat sink. Shown in cross-section in Figure 2-5, the two L-shaped halves of the 2.25 mm square, 18 cm long alumina waveguide are sandwiched between alumina spacers and aluminum headers. This assembly fits snugly in the stainless steel vacuum envelope and an external heat sink then compresses the structure together. Thermal contact between these components is enhanced by lapping their surfaces together. The symmetrical cooling of the discharge structure should result in enhanced mode stability at high input power densities.

A single waveguide section is shown in closer detail in Figure 2-6. The thick sides are designed to allow the conduction of heat away from the side walls of the waveguide, into the ceramic spacers, as well as directly through the thin top and bottom walls. Seventeen 0.5 mm by 1.0 mm channels are placed at 1 cm intervals along the length of the waveguide to enhance the exchange of gases between the discharge and the gas ballast. Each channel is plated with a platinum film thus providing a distributed catalyst which should reduce equilibrium CO_2 dissociation levels.

The active discharge length of the lasers is extended to 17 cm (from 15 cm in the soft-sealed laser) in order to increase the maximum power output.

Figure 2-5

Cross-section through the Hard-Sealed Laser

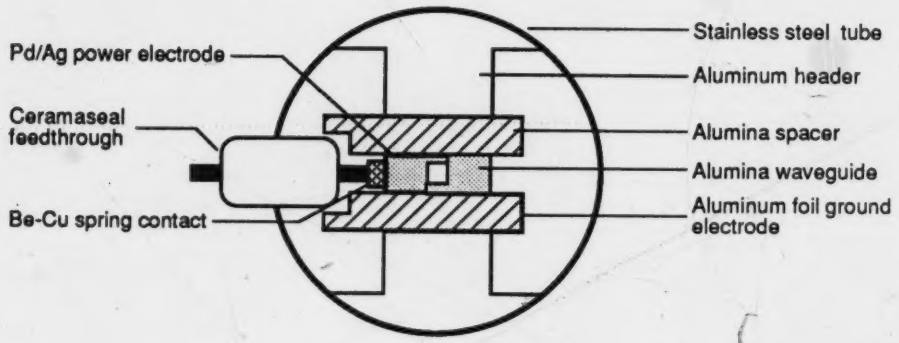

Figure 2-6

Hard-Sealed Laser
Waveguide Structure

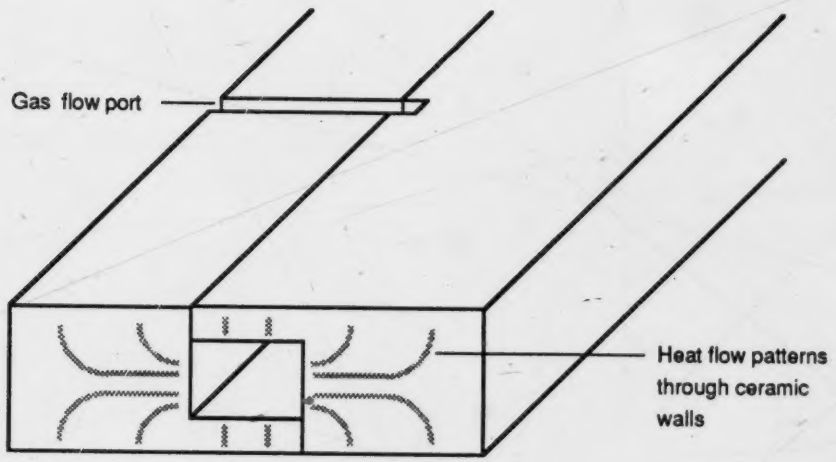

This is the maximum discharge length achievable with a single resonating inductor which still maintains a 5% voltage variation along the channel. The electrodes are capacitively coupled through the 1 mm thick waveguide walls. The power electrode consists of a metallized Pd/Ag thick film while the ground electrode is a 0.025 mm thick aluminum foil which wraps around its adjacent ceramic spacer to make contact with the aluminum header. The main function of the ceramic spacers is to isolate the power electrode from the grounded aluminum headers. The extensions on the spacers prevent breakdown between the electrical feedthrough and the headers. The power electrode is completely buried except for a small tab where external electrical contact is made. The spacer on the ground side is not necessary electrically, but was included to preserve the thermal symmetry of the structure. A Ceramaseal fitting is used for the electrical feedthrough, and contact with the tab on the waveguide is maintained by a compressed gold-plated beryllium-copper spring.

Special attention was paid to the materials chosen for the hard-sealed lasers. All ceramic parts are to be fabricated from high thermal conductivity 99.5% alumina. High-purity alumina has the additional advantages of low porosity and it can be polished to a high surface finish. Aluminum was chosen for the headers because of its light weight and high thermal conductivity. The external tube and optical end flanges will be fabricated from stainless steel as it is the most suitable material for welding and brazing.

The optical flanges in the hard-sealed laser are much more compact than those in the soft-sealed laser. They use a three-point deformed metal adjustment with crushed indium gaskets to seal the 3/8" ZnSe optics in place. Interaction between the discharge and the optics is minimized by locating the optical mounts 2 mm away from the ends of the waveguide and leaving 5 mm

of dead space at each end of the waveguide. Efforts have also been made to reduce the convective flow of gas past the optics by the introduction of stainless steel baffles, butted up against each end of the waveguide, which will isolate the optical mounts from the main gas ballast.

CHAPTER 3

DESIGN OF A LASER PROCESSING STATION FOR LIFETIME EXPERIMENTS

The construction and study of sealed CO_2 waveguide lasers first required the assembly of experimental apparatus. The core of this equipment was an integrated vacuum/gas analysis station for the processing of assembled laser tubes and the analysis of laser gas composition during subsequent lifetime experiments. The key components of this system included a hydrocarbon-free cryogenic pump and a residual gas analyzer. In the following sections techniques for measuring laser gas composition, gas sampling methods, and the design and calibration of the vacuum/gas analysis station are all considered.

3.1 The Measurement of Laser Gas Composition

A number of different techniques can be used to analyze the gas composition of sealed CO_2 lasers. Those which have appeared most frequently in the literature include infrared absorption spectroscopy, visible emission spectoscopy, mass spectrometry, and gas chromatography. The technique chosen for this study had to be capable of measuring the relative concentrations of all gases expected to be present in a sealed CO_2 waveguide laser. These included the four primary laser gases: carbon dioxide, nitrogen, helium, and xenon, the dissociation products: carbon monoxide and oxygen, and the contaminants: water vapor and hydrogen. Detection limits for trace contaminants were set at 100ppm (or 0.01%). This was low enough to measure the presence of contaminants before laser output power was affected (water vapor levels of 0.1% have been reported to inhibit laser action[27]) without requiring expensive analytical equipment. Gas composition measurements

were not permitted to disturb the operation of the laser. Response time was not considered to be an important factor in the design of equipment for long-term tests. Except during the first few hours of operation, significant changes in gas composition occur over a period of tens of hours. The analysis technique finally had to be integrated into the laser processing station and at a feasible cost.

A major advantage of the two optical techniques is that they do not require the removal of any gas from the laser. This is a very important factor in sealed waveguide lasers because of their small gas ballast volume. Also, an essentially unlimited number of measurements can be made. The response time of optical techniques is very fast because these techniques are based on optical processes which have submicrosecond time constants. Infrared absorption spectroscopy, based on the absorption of infrared light by the excitation of molecular vibrational and rotational states, has been used to measure the concentrations of both CO_2 and CO molecules in laser gas mixtures. Gasilevitch[45] has used a two-beam system in which a measuring beam (with a wavelength of 4.27μ for the detection of CO_2 and 4.02μ for the detection of CO) was passed through the gas mixture and its intensity compared with that of a reference beam. Measurement accuracy was quoted at ±0.5% for CO_2 and ±5% for CO. Infrared absorption spectroscopy is not well suited to gas composition analysis in a working discharge. The presence of excited species in the glow discharge results in infrared absorption which is no longer proportional to gas concentration. Gasilevitch performed the majority of his experiments on flowing gas lasers with gas measurements made immediately after the gas left the discharge tube. Measurements on sealed lasers were made only after the discharge was extinguished.

In visible emission spectroscopy the light emission from the glow dicharge is used to measure the concentrations of constituent gases. As different atomic and ionic species emit light at specific wavelengths, gas concentrations can be measured by monitoring light intensity using a monochromator. This technique has been widely used in conventional DC discharge CO_2 lasers because their glass tube construction permits visible light to be monitored from the side of the tube without interfering with the infrared emissions along the optical axis of the laser. Most researchers have used this technique to measure only a limited number of gases in the discharge, most notably the CO bands, at 4835Å[10] and 5198Å[46]. Visible emission spectroscopy is more difficult to apply to waveguide lasers because the waveguide is opaque and is often contained in a metal vacuum envelope.

The most commonly used gas analysis technique for CO_2 laser discharge chemisty has been mass spectrometry. It has been used in investigations of DC-excited CO_2 discharges[10,47], direct sampling of sealed and flowing gas DC-excited conventional CO_2 lasers[14,12,48], sealed TEA CO_2 lasers[49,50], sampling of DC-excited waveguide CO_2 lasers[27,51,19], RF-excited CO_2 discharges[52,22], and more recently in RF- excited CO_2 waveguide lasers[23]. Flowing gas systems are normally sampled continuously and sealed systems use periodic sampling. Mass spectrometers typically consist of an ionizer, a mass separator, and an ion detector. Gas molecules are first ionized by 70eV electrons (most gases have broad maxima in their total ionization cross sections in the energy range of 70-100eV) after which the ions are focussed and accelerated toward the mass separation stage. Mass separation is based on the ratio of the ions mass to electric charge. Only ions within a narrow range of m/e are able to pass into the ion detector. Although almost a dozen techniques for

mass separation have been developed, the two systems most commonly found in commercial instruments are the magnetic sector analyzer and the rf quadrupole analyzer (for a discussion of these two techniques see Drinkwine[58]). The class of mass spectrometers most suited to the analysis of CO_2 laser gas mixtures are referred to as residual gas analyzers (RGAs). These are compact, relatively inexpensive instruments capable of scanning mass ranges between 1 and 100 to 300 amu with a dynamic pressure range of 5 orders of magnitude. Response times for mass spectrometry are largely dependent on gas sampling techniques but can vary from milliseconds to minutes. A more detailed discussion of gas sampling follows in the next section.

Gas chromatography has also been used a number of times, for the analysis of TEA laser gas mixtures[53,54] and RF discharges in CO_2[55]. This technique is based on the principle that gases can be separated by passing them through a column packed with a material that has an affinity for one or more of the gas components. The more strongly a gas is adsorbed by the packing the more slowly it moves through the column. Different gases can be identified by the characteristic times it takes for them to travel through the column. Gas chromatography has one major advantage over mass spectrometry in that the peaks for nitrogen and carbon monoxide do not overlap each other (as is the case in mass spectrometry) and so the concentrations of these gases can be determined with greater accuracy.

After considering the four analytical techniques discussed above, mass spectrometry was chosen for the following reasons:

(1) Mass spectrometry is a proven technique with the capability of detecting all gases of interest in the sealed CO_2 laser discharge.

(2) The waveguide laser design, with an opaque alumina waveguide, precludes the use of sidelight emission measurements. Moreover, visible emission spectroscopy has not been shown to be capable of detecting all of the gases of interest.

(3) Infrared absorption spectroscopy was unsuitable for long term lifetime measurements because measurements could not be taken during the discharge.

(4) The construction of sealed lasers required a vacuum station for the evacuation, filling, and leak testing of laser tubes. The RGA, with its leak detection and pressure measurement capabilities, was essential equipment for a laser processing station. A gas chromatograph would have been an extra expense.

3.2 Gas Sampling Techniques

Gas chemistry studies and lifetime tests required small samples of gas to be withdrawn from the laser for analysis in the RGA. It must be stressed that laser gas composition was determined indirectly as it was the gas composition inside the RGA chamber which was being analyzed and not the gas inside the laser itself. Gas sampling techniques then became of critical importance to the accuracy of gas composition analysis.

A number of factors had to be considered before a suitable gas sampling technique was chosen. First, it was important that gas sampling not significantly decrease the gas pressure inside the laser. A maximum of 1% of the total gas ballast was permitted to be removed by sampling. The gas sampling system also had to introduce a large pressure differential between the laser and the RGA chamber because the maximum operating pressure for an RGA is typically

only 10^{-4} torr. This could be achieved by using one of the two differential pumping methods shown in Figure 3-1.The first method utilizes a low conductance aperture and a single vacuum pump which maintains a constant flow of gas through the RGA chamber[36]. The second method uses two apertures and a second pump to bypass most of the gas flow away from the RGA chamber. This allows the collisionless expansion of the gas into the RGA chamber with minimal changes in gas composition and fast gas sampling time constants[47]. Unfortunately the latter technique consumes large quantities of gas and so was not suited to sampling sealed lasers with small gas volumes. Single aperture differential pumping was thus chosen as the gas sampling method.

A simple analysis was used to determine the gas flows in single aperture differential pumping as shown in the expanded sketch of Figure 3-2. It was important to choose component values which minimized any mass dependencies which could result in gas composition changes. The gas pressure in the laser is given by p_{laser}, p_{rga} is the pressure in the RGA chamber, and p_p is the pressure in the pump, whose speed is S_p. The two conductances C_1 and C_2 connect the laser to the RGA chamber and the RGA chamber to the pump. As the gas flow through the system is the same in each section, the following relation holds (assuming no outgassing in the system)

$$Q_{leak} = C_1(p_{laser} - p_{rga}) = C_2(p_{rga} - p_p) = S_p p_p$$

Eliminating p_p,

$$p_{rga} = \frac{p_{laser}}{1 + \left(\frac{C_2}{C_1}\right)\left(\frac{S_p}{S_p + C_2}\right)}$$

Under molecular flow conditions both conductances C_1 and C_2 have a mass dependency of $m^{1/2}$. Also depending on the type of pump used, there can be

Figure 3-1

Pump Configurations for Laser Gas Sampling

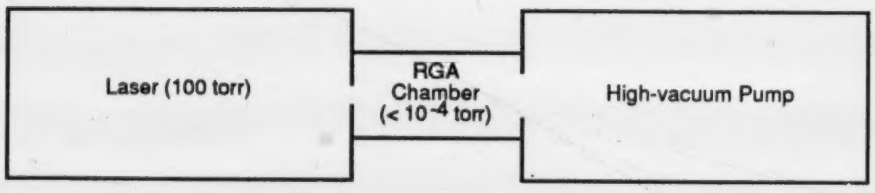

Single Aperture Differential Pumping

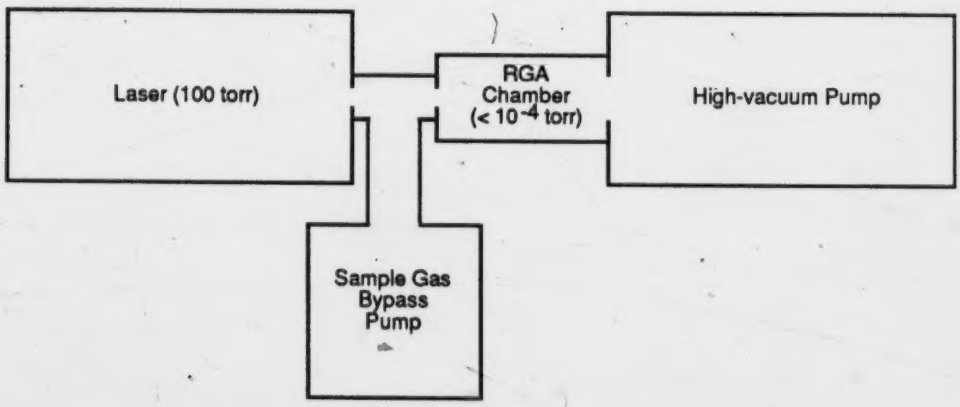

Dual Aperture Differential Pumping

Figure 3-2

Gas Flows in Single Aperture Differential Pumping

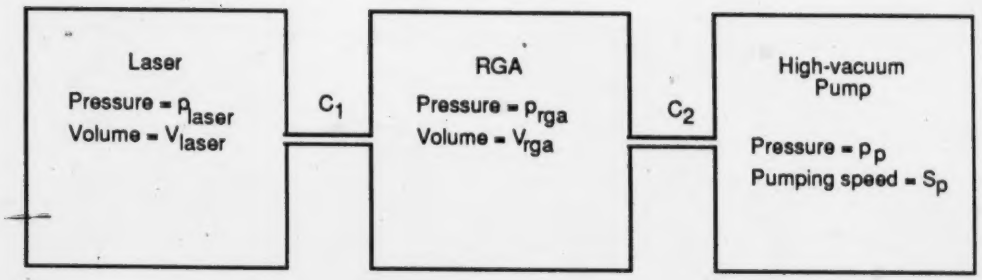

mass dependencies in the pumping speed, S_p. Thus single aperture gas sampling can cause significant gas composition changes. However if the pumping of the RGA chamber is conductance limited such that $C_2 << S_p$, then

$$p_{rga} \approx \frac{p_{laser}}{1 + C_2/C_1}$$

and the mass dependencies of C_1 and C_2 will cancel each other out.The gas composition changes induced by single aperture sampling can thus be minimized.

The necessary conductance of the gas sampling aperture, C_1, was calculated by first estimating the maximum allowed quantity of gas removed in a single sample. Assuming that

(i) the laser gas ballast volume = 0.1 litre,

(ii) the laser gas pressure = 120 torr,

(iii) a maximum of 50 samples will be taken (This corresponds to roughly one sample per day over a 1000 hour testing period),

(iv) a maximum of 1% of the laser gas is removed during sampling,

(v) the gas sampling time is 300s.

The leak rate is then equal to

$$Q_{leak} = \frac{(12 \text{ torr-l})(0.01)}{(40 \text{ samples})(300\text{s})} = 1.0\text{x}10^{-5} \text{ torr-l/s}$$

Now assumimg $p_{rga} << p_{laser}$,

$$C_1 = \frac{Q_{leak}}{p_{laser}} = 8.3\text{x}10^{-8} \text{ l/s}$$

As this is a very small conductance it was most easily achieved through the use of a precision leak valve.

System component values also determined the gas sampling time constant. As shown by Sullivan and Buser[56], the gas sampling time constant in

the single aperture system is equal to V_{rga}/C_2 (where V_{rga} is the volume of the gas analyzer chamber). This can be minimized either by reducing V_{rga} or by increasing C_2. However it has just been shown that C_2 must be minimized to prevent gas composition changes. Generally there is a value of C_2 which will best satisfy both gas composition and time constant constraints.

3.3 Laser Processing Station Design

The requirements for a vacuum/gas analysis system are best described by considering the sequence of operations to be carried out when processing and testing a sealed waveguide laser. The assembled laser is first tested for leak tightness in order to meet six month shelf life requirements. Vacuum baking at temperatures not likely to exceed 150°C is then used to remove residual gas contaminants. During this phase the residual gas composition must be monitored in order to determine the types and relative outgassing rates of background contaminants. This information may then point to improvements in materials or assembly techniques. After processing, the laser tube is backfilled with a mixture of high purity gases to a total pressure of approximately 120 torr. The partial pressure of each gas component should be measured with an accuracy of ±0.1 torr. Gases should be mixed in the vacuum station (rather than by introducing a premixed gas) as it will be necessary to experiment with a variety of gas mixtures.

Lifetime testing, during which the laser is operated continuously for an extended period of time (or until the output power has dropped below a predetermined threshold), can then begin. At periodic intervals, gas samples are removed from the laser and analyzed for changes in composition using an

on-line mass spectrometer. Gas sampling must not perturb the laser gas pressure significantly as this can influence the laser's output power.

The vacuum/gas analysis station requirements can thus be summarised as follows:

(1) A residual gas analyzer (RGA) is required for leak detection, background contamination analysis during tube processing, and laser gas composition analysis during lifetime testing.

(2) Laser gas samples are to be introduced into the RGA using a variable leak valve in a single aperture differential pumping scheme. Component values were chosen to minimize sampling-induced gas composition changes and perturbation of laser gas pressure.

(3) High-purity gases are to be mixed accurately (±0.1 torr) and introduced into the laser without contamination at total pressures of 80 to 150 torr.

(4) The vacuum station must not introduce contamination into the laser during processing.

(5) Background contamination levels in the vacuum system need to be minimized so as to allow accurate analysis of the laser gases.

(6) Gas pressure in the station may be cycled regularly between atmospheric (700 torr) and high vacuum but it is desirable that the background contamination levels required for analysis be achieved with overnight baking of the system. The RGA must be connected to the main system through a valve which can be closed during high pressure operations.

(7) The above requirements must be met with a single high vacuum pump so as to minimize system costs.

Using these requirements, the laser processing station shown in Figure 3-3 was designed and assembled. A block diagram and list of all major components is shown in Figure 3-4. The system was designed around a 5 litre stainless steel chamber whose main function, other than structural support, was for gas mixing. The high-vacuum pump selected for the system was a 350 l/s cryopump (CTI-Cryogenics model Cryotorr 100). A 0.8 l/s direct-drive rotary pump (Edwards model E2M2) with an activated alumina oil-vapour trap was connected both to the chamber and the cryopump for roughing purposes. Instru - mentation included a residual gas analyzer (Spectrum Scientific model SM100D with dual Faraday cup/secondary electron multiplier detectors) for total pressure measurement from 10^{-4} to 10^{-11} torr, partial pressure analysis, and leak-testing, a capacitance manometer (Vacuum General model CML-1000) with a range of 1000 to 0.1 torr for gas mixing, and a pirani gauge (Edwards model 14) with a useful range of 1.0 to 10^{-4} mbar for monitoring pumpdown.

The system was designed to provide minimum turnaround time between high-pressure laser backfilling operations and high-vacuum gas analysis operations. During backfilling ~100 torr of high-purity gases were introduced into the gas mixing chamber through two-stage regulators (Matheson model 3104) and measured with an accuracy of ±0.1 torr using the capacitance - manometer. A six line gas manifold allowed the simultaneous connection of the four primary laser gases (helium, carbon dioxide, nitrogen, and xenon), a commonly used premixed gas (6:1:1 of $He:CO_2:N_2$), and a gas mixture for calibrating the gas analyzer. Both the cryopump and gas analyzer were valved off from the gas mixing chamber during this procedure.Two lasers are shown

Figure 3-3

The Laser Processing Station

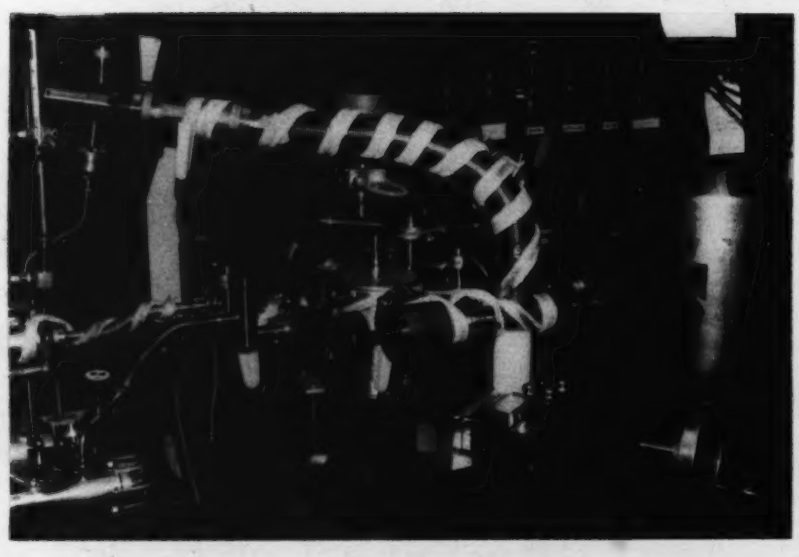

Figure 3-4

Block Diagram of the Laser Processing Station

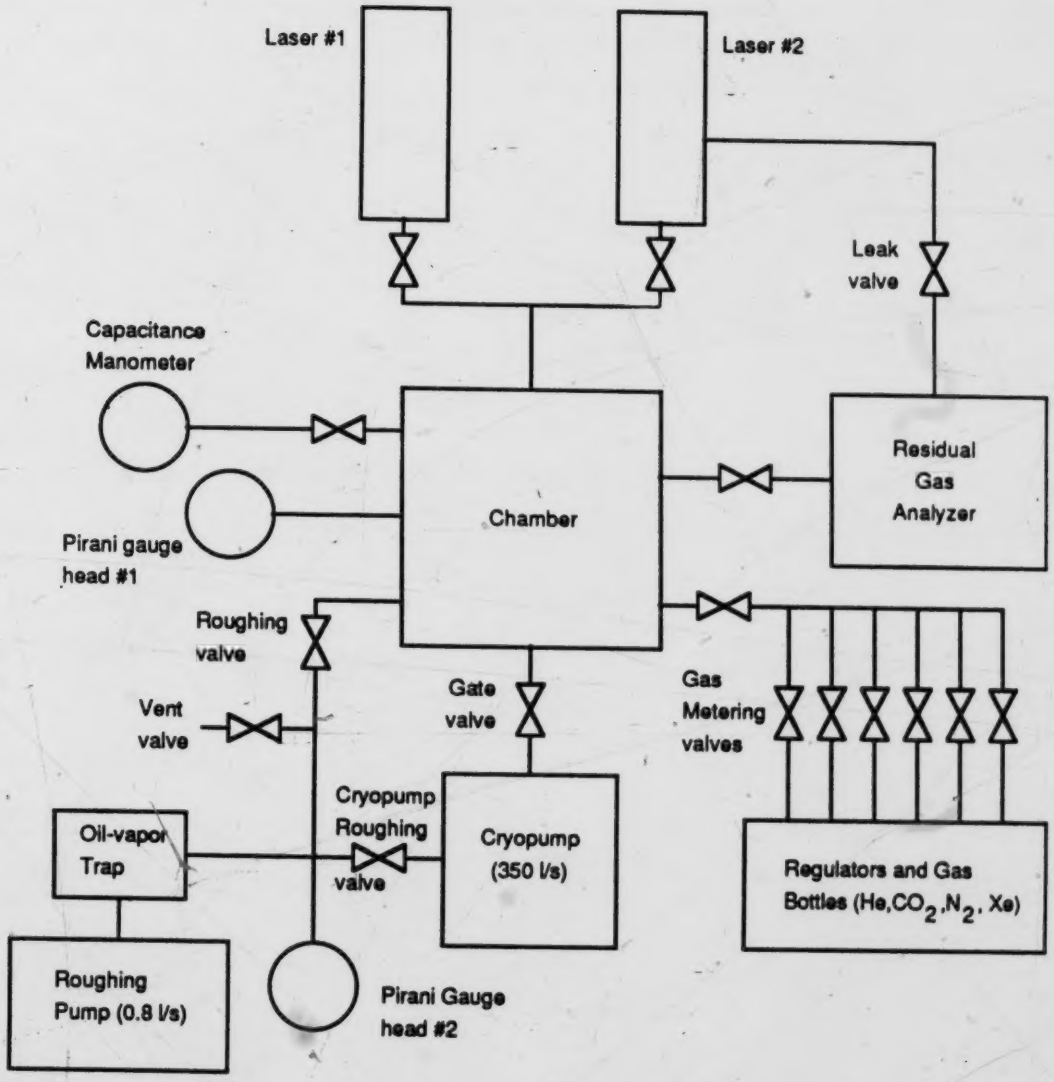

connected to the chamber, each by a separate valve. This allowed one port to be used for lifetime testing and another for backfilling of lasers during day-to-day testing.

During laser gas analysis the RGA chamber was pumped down to a base pressure of $5x10^{-9}$ torr. This was achievable with overnight pumping. Gas samples from the laser were introduced through a precision leak valve (CVT model VML/14) at a total pressure of $5x10^{-7}$ torr.

The ability to produce clean high-vacuum conditions was one of the main criteria in the choice of specific system components such as the cryopump, valves, and fittings. Cryogenic pumping is exceptionally clean as it is based on the condensation of gases on surfaces which are cooled to less than 10°K. The cryopump chosen for this system was cooled by a closed-cycle helium refrigerator. Because cryopumping is completely oil-free and does not require a backing pump, there was no possibility of hydrocarbon backstreaming from the pump into the system, consequently there was also no need for a cold-trap. The only source of hydrocarbon contamination in the system was the rotary pump, which is only required when roughing the chamber or during cryopump start-up. The Cryoto.. 100 cryopump was limited to a maximum gas burst of 40 torr-l,so the 5 litre chamber had to be pumped down to at least 8 torr before the high-vacuum valve could be opened. This is a relatively high crossover pressure (by high-vacuum pumping standards) and there was little chance of contamination from the roughing pump, first because pumping from atmospheric pressure (700 torr) to 8 torr was achieved in under 10 seconds, and secondly because the system remained in the viscous flow regime throughout the entire roughing period.

Two potential problems with cryopumping were considered before the pump was chosen. First, a cryopump can only pump very limited quantities of helium, after which the cold-head temperature will increase and the pumping capacity for other gases can be impaired. Helium levels far in excess of the pump's capacity were found in the chamber following laser backfilling. This problem was solved by purging the chamber with dry nitrogen after backfilling. The helium load introduced during gas sampling was also considered.The total quantity of sampled gas, which is nominally 60% helium, contained 0.072 torr-l of helium. Although there are no figures available for the Cryotorr-100 pump, the stated capacity for a cryopump with similar specifications (Balzers model RKP101) was 11.25 torr-l, thus no problems were anticipated in handling the helium load from gas sampling.

A second problem concerned the ability of the cryopump to withstand the heat load from bakeout. In order to achieve high-vacuum operation in an otherwise clean, leak-free vacuum system it was necessary to bake the system out to reduce the outgassing rate of adsorbed gases, most notably water vapour. For example, following a 20 hour bakeout at 150°C the water vapour outgassing rate of type 304 stainless steel can be reduced from 10^{-10} torr-l/(cm^2 s) to 10^{-16} torr-l/(cm^2 s)[63]. A study of a baked cryopumped system by Kubiak[57] demonstrated that chamber temperatures of 170°C could be tolerated before a significant release of adsorbed gas occured from the second stage cryopanel. By using a thermal baffle, placed between the pump and the chamber, bakeout temperatures exceeding 200°C were achieved. Thus no problems were anticipated in baking out the system to 150°C.

Valves and fittings for all parts of the system except the roughing and gas input sections were chosen to meet high-vacuum standards. Stainless-steel

bellows-sealed valves with low-outgassing viton O-ring seals were used exclusively throughout the system and all fittings were of stainless-steel with ultra-high-vacuum Conflat flanges and copper gasket seals. The chamber, which was designed and constructed at the University, was of TIG-welded stainless-steel construction with Conflat flanges. Inside welds, which eliminate virtual leaks caused by trapped gas, were made wherever possible. The inside surface of the chamber was also electropolished to reduce outgassing. The roughing section used medium-vacuum KF fittings and high-conductance flexible stainless-steel lines. The gas handling section, although not required to meet high-vacuum standards, was expected to deliver research-grade gases to the lasers with minimal contamination. As a result the six line gas manifold was constructed of glass because it was felt an alternative design using brazed stainless tubing would have been very difficult to clean. Stainless-steel gas regulating valves were used on the six gas inlet lines and all connections were made with stainless-steel Swagelock fittings.

After initial leak-testing, the assembled system was baked out for 48 hours at 120°C. The capacitance manometer, which could withstand a maximum temperature of only 45°C, was thermally isolated by a valve and a water-cooled clamp during bakeout. Following bakeout a base pressure of 4×10^{-9} torr was obtained. A partial pressure scan of the system is shown in Figure 3-5. The largest peak, at mass 18, was water vapour. Higher temperature baking, which would reduce this peak, was not used because the system was being frequently cycled between atmospheric and high-vacuum conditions. Also, discharge tests resulted in significant quantities of water vapour being formed inside the lasers, some of which was subsequently transferred into the vacuum system. Other mass peaks were from a small air

Figure 3-5

Residual Gas Analysis
of Laser Processing Station

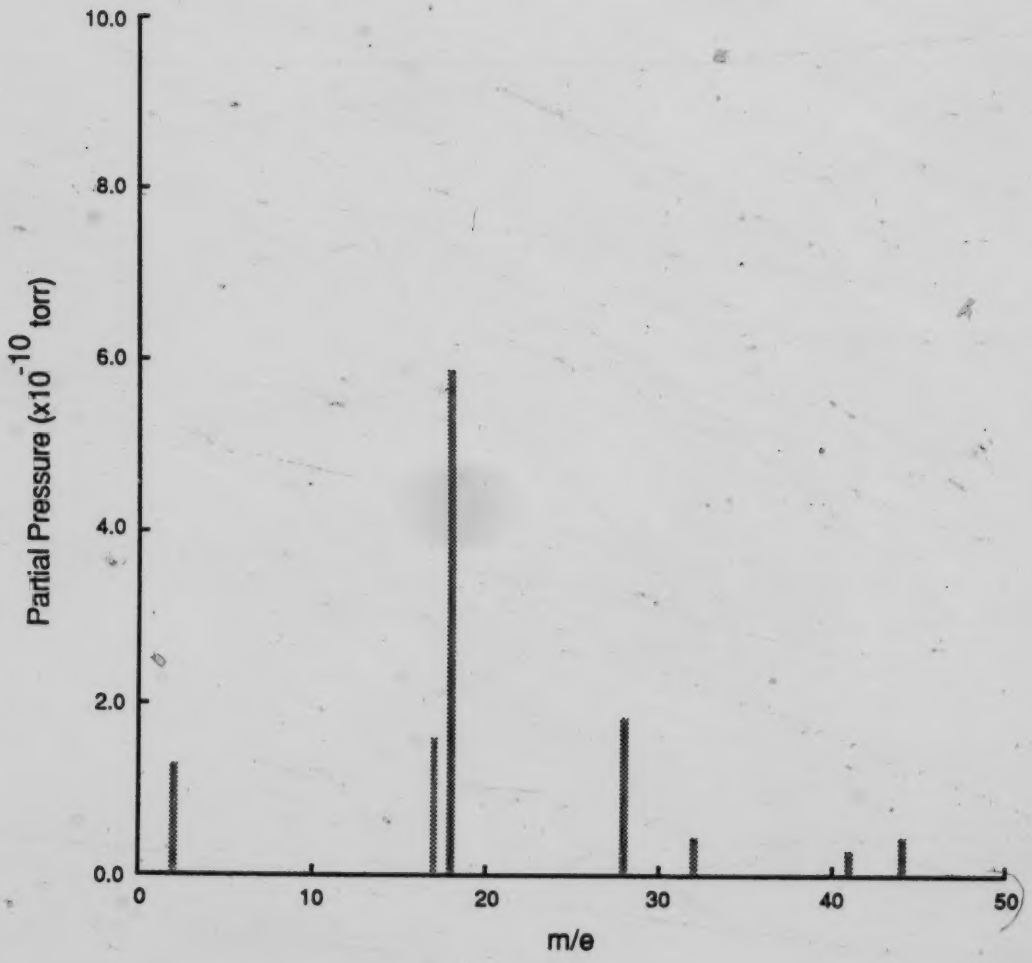

leak(masses 28 and 32), hydrogen(mass 2) and CO_2(mass 44). Total hydrocarbon levels, which can be estimated by the mass 41 and 43 peaks, were less than 0.2×10^{-10} torr, and no traces of roughing pump oil at masses 55 and 57 were detectable.

3.4 Gas Analyzer Calibration

Quantitative analysis of gas composition using a residual gas analyzer was not straightforward and required careful calibration. Much of the difficulty resulted from the process in which the sample gas is ionized. As explained in section 3.2 the gas sampling process can first affect the analysis by inducing changes in gas composition caused by mass dependencies in conductance and pumping speeds. Gas molecules entering the RGA are then ionized by collisions with 70eV electrons. This results in additional complicating factors. First, ionization efficiency varies strongly from gas to gas as shown in Table 3-1. Moreover, quoted ionization efficiencies are nominal values which depend on filament type and will change as the filament ages. Secondly, 70eV electrons have sufficient energy to cause dissociative ionization and the formation of higher ionization states[47]. The output for a given gas then consists of a series of peaks, called a cracking pattern, which represents the mass-to-charge ratio of each molecular fragment. If several gases are present in the system, it is not uncommon that the peaks of one gas overlay the peaks of another. Cracking patterns are tabulated for a large number of gases but again represent only nominal values. The gas flow conditions in the RGA chamber, chemical reactions between the ionized species, linearity of the mass filter (the mass filter linearity in an RF quadrupole RGA is highly dependent on focus, energy, and resolution settings) and the ion detector can all induce significant changes in the relative peak heights of the cracking pattern. The problem is then to relate a

Table 3-1

Ionization Efficiency of Laser Gases[59]

Gas	H_2	He	H_2O	CO	N_2	O_2	CO_2
Relative Sensitivity	0.7	0.23	1.17	1.09	1.00	0.62	0.9

series of peaks, many of which contain the contributions of more than one gas, to the partial pressures of gases in the laser. The accurate measurement of the partial pressures of gases using the RGA required three crucial steps: (i) the measurement of cracking patterns for each gas of interest, (ii) the use of the cracking patterns to separate overlapping peaks, and (iii) calibration against a gas mixture of known composition.

Cracking patterns were measured experimentally for three gases: N_2, CO_2, and CO. All measurements were performed by filling the soft-sealed laser tube with 100 torr of ultra-high-purity gas and then pumping the system down to a base pressure of less than 10^{-8} torr. The laser was pumped and baked between tests. For each cracking pattern at least two measurements were taken at up to seven different sampling pressures between $1x10^{-8}$ and $5x10^{-7}$ torr. This covered the pressure range over which the gases were observed at the total sampling pressure of $5x10^{-7}$ torr. The results of the cracking pattern measurements are summarized in Table 3-2. All values are expressed as a percentage of the principal peak height. Standard deviations were generally from 3 to 5% which was judged to be acceptable. Higher standard deviations were recorded at the lower sampling pressures. A pressure dependency was observed in the cracking patterns as shown in Figures 3-6 and 3-7. There was a general trend toward a decrease in the ratios at higher sampling pressures. For all analyses cracking coefficients were calculated by using a linear interpolation of the pressure curves.

Interpretation of RGA data was performed using the method outlined by Drinkwine[58]. In this method the partial pressure of a gas is related only to the height of the largest, or principal, peak in its cracking pattern. The use of this method is best explained by illustration with the sample analysis of a typical

Table 3-2

Cracking Coefficients for N_2, CO, and CO_2

Gas: N_2 Principal Peak: mass 28

Peak (m)	Partial pressure of principal peak (P)	Ratio m/P
14	1.0×10^{-8}	0.0757 ± 6.5%
	2.5×10^{-8}	0.0801 ± 1.9%
	5.0×10^{-8}	0.0805 ± 1.2%
	7.5×10^{-8}	0.0794 ± 6.8%
	1.0×10^{-7}	0.0781 ± 1.8%
	2.5×10^{-7}	0.0753 ± 0.6%
	5.0×10^{-7}	0.0723 ± 1.4%
29	1.0×10^{-8}	0.0114 ± 17.6%
	2.5×10^{-8}	0.00864 ± 2.7%
	5.0×10^{-8}	0.00910 ± 4.6%
	7.5×10^{-8}	0.00815 ± 7.1%
	1.0×10^{-7}	0.00802 ± 1.1%
	2.5×10^{-7}	0.00759 ± 7.8%
	5.0×10^{-7}	0.00817 ± 3.5%

Gas: CO_2 Principal Peak: mass 44

Peak (m)	Partial pressure of principal peak (P)	Ratio m/P
12	1.0×10^{-8}	0.05524 ± 8.0%
	5.0×10^{-8}	0.04952 ± 2.5%
	1.0×10^{-7}	0.04662 ± 2.4%
	5.0×10^{-7}	0.04575 ± 4.7%
16	1.0×10^{-8}	0.07667 ± 8.3%
	5.0×10^{-8}	0.06806 ± 2.6%
	1.0×10^{-7}	0.06409 ± 2.7%
	5.0×10^{-7}	0.06440 ± 2.4%
28	1.0×10^{-8}	0.180 ± 14%
	5.0×10^{-8}	0.09973 ± 2.8%
	1.0×10^{-7}	0.09181 ± 1.7%
	5.0×10^{-7}	0.08920 ± 2.3%

Gas: CO Principal Peak: mass 28

Peak (m)	Partial pressure of principal peak (P)	Ratio m/P
12	1.0×10^{-8}	0.03698 ± 4.2%
	5.0×10^{-8}	0.03504 ± 5.2%
	1.0×10^{-7}	0.03487 ± 1.8%
	5.0×10^{-7}	0.03196 ± 2.8%

Figure 3-6

Cracking Coefficients vs Pressure for N_2 and CO

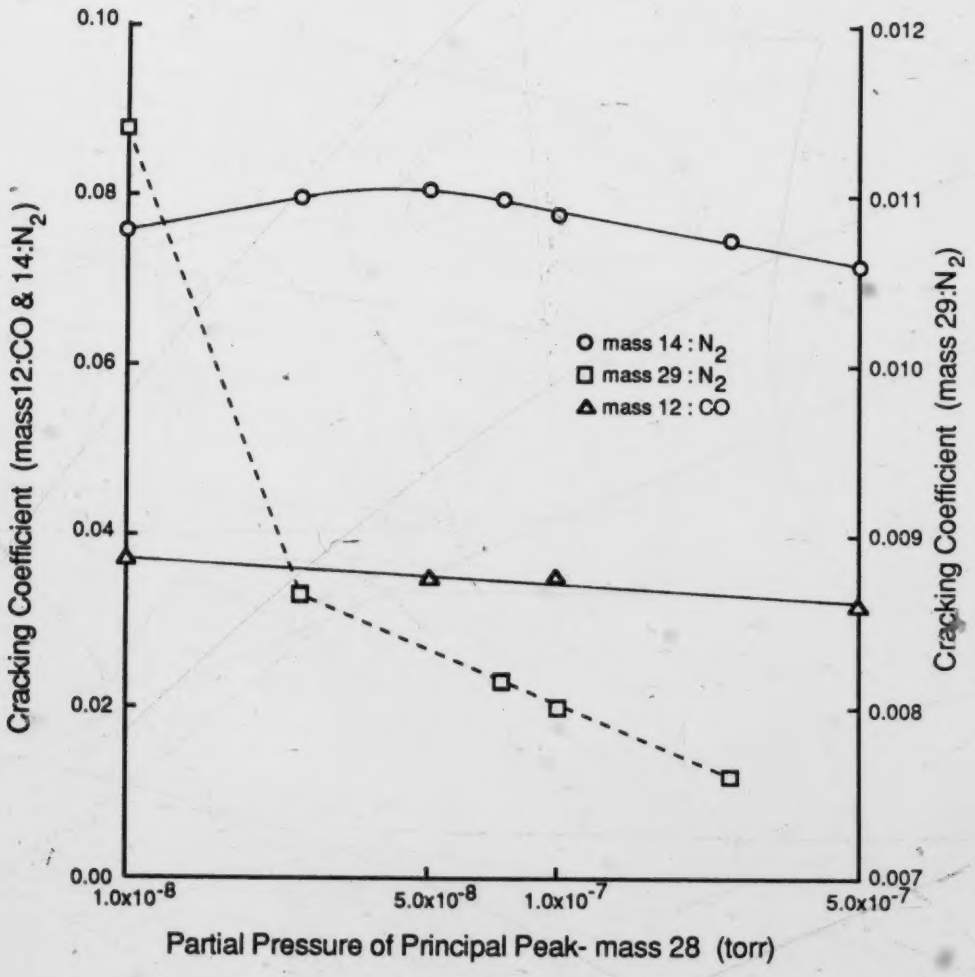

Figure 3-7

Cracking Coefficients vs Pressure for CO_2

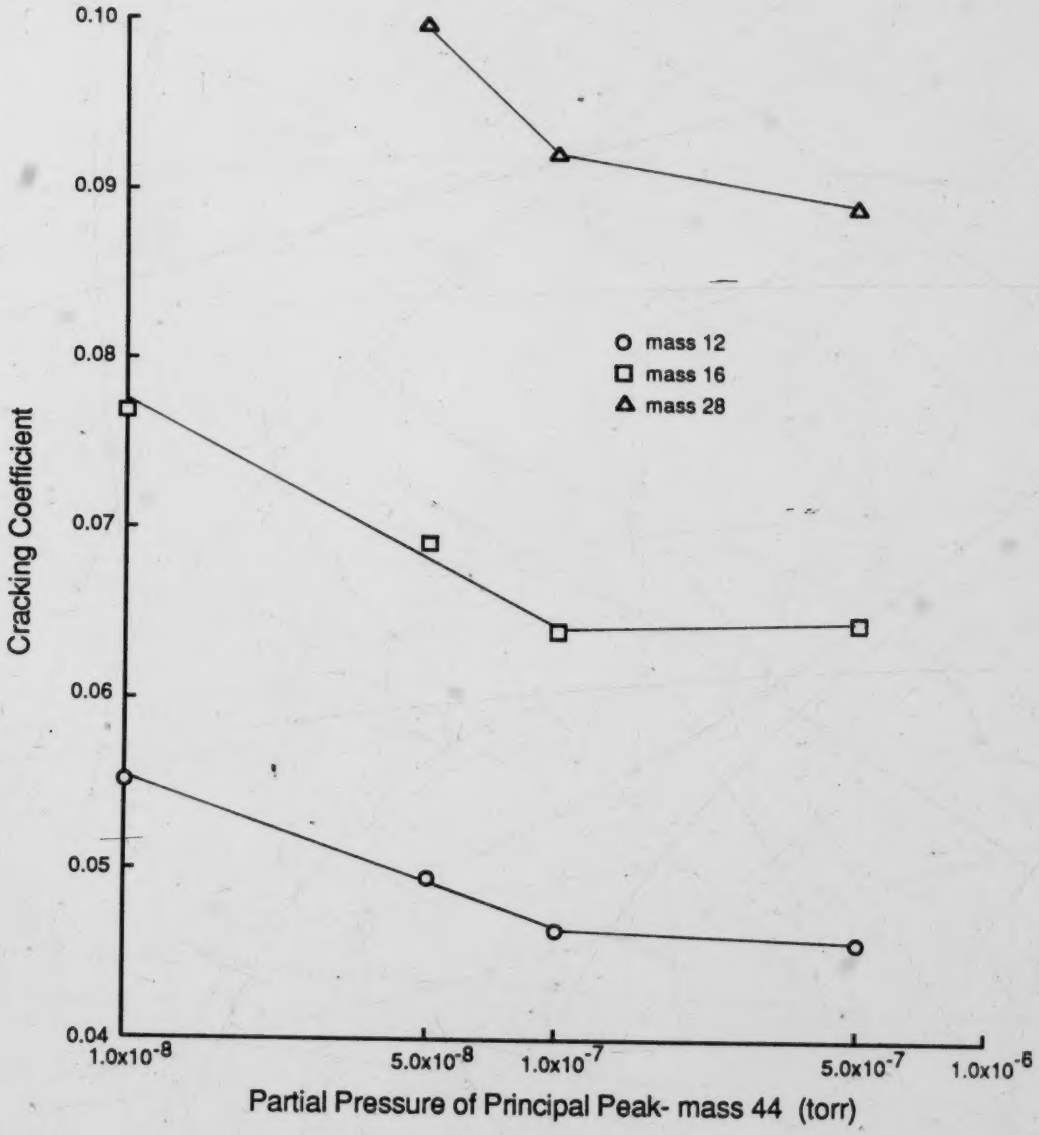

CO_2 laser gas mixture. A mass scan of a gas sample obtained from the 15cm laser following a 22 hour discharge test is shown in Figure 3-8 (The background from the RGA chamber has been subtracted off). The gases of interest on the scan are: the original laser gases (CO_2, N_2, He, and Xe), the CO_2 decomposition products (CO and O_2), and trace contaminants (H_2 and H_2O). The sequence of operations used to obtain the principal peak heights is shown in Figure 3-9.This technique was used for almost all subsequent analyses of CO_2 laser gas mixtures. First, the principal peak heights for He, H_2O, O_2, CO_2, and Xe[60] (at masses 4,18,32,44, and 64.5) can be measured directly. The principal peak heights for the remaining gases are calculated using cracking patterns. The principal peak for CO is obtained by subtracting the CO_2 contribution off the mass 12 peak, and using the resulting CO peak at mass 12 to calculate the principal peak at mass 28. The nitrogen peak is obtained in either of two ways. First, the secondary peak at mass 14 can be used to calculate the principal peak at mass 28 (the CO contribution at mass 14 is typically so small that it can be ignored). Alternatively, the CO_2 contribution at mass 28 can be calculated and along with the CO contribution at mass 28 be subtracted off to leave the remaining N_2 principal peak. The method outlined above will not work in situations where there are no peaks which can be measured directly, in which case a least squares analysis[61] can be used.

Using the procedure for calculating principal peaks and the measured cracking patterns, the RGA was first calibrated against an analyzed five-component gas mixture (Matheson Primary Standard[62]) containing N_2, CO_2, CO, O_2, and He. Calibration was performed by filling the 15 cm laser with 100 torr of the reference mixture. Five mass scans were recorded at a gas sampling pressure of $5x10^{-7}$ torr. Principal peak heights for the five gas

Figure 3-8

Mass Scan of a Representative Laser Gas Sample

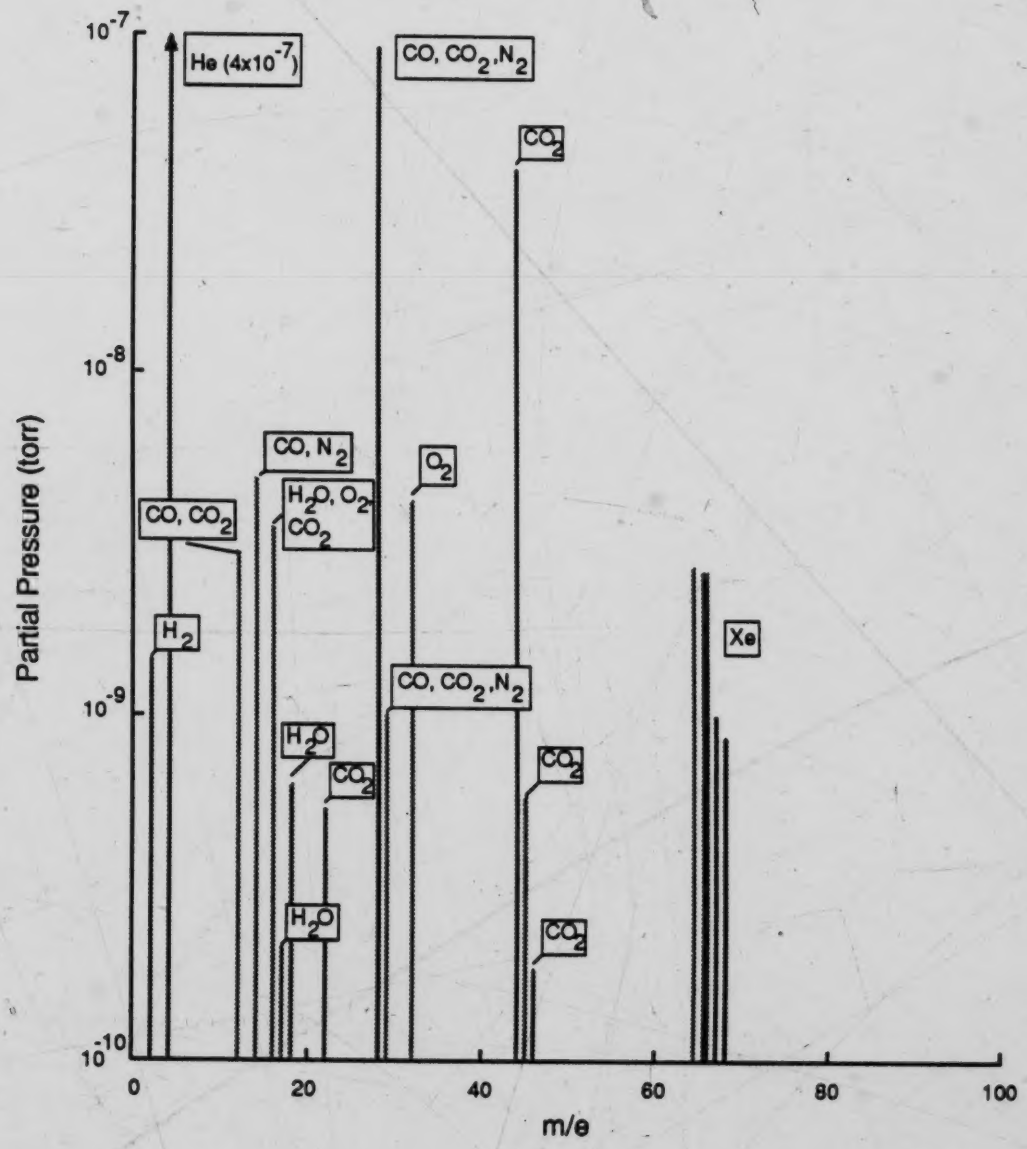

Figure 3-9

Separation of Principal Peaks in a Laser Gas Sample

1.0 Record raw data (with RGA background already subtracted off) from Figure 3-8. Principal peaks with no interference (denoted below by an asterisk) can be recorded directly.

m/e	Peak Height	Description
2*	1.45×10^{-9}	H_2
4*	4.0×10^{-7}	He
12	3.02×10^{-9}	CO, CO_2
14	4.92×10^{-9}	CO, N_2
18*	6.3×10^{-10}	H_2O
28	9.2×10^{-8}	CO, CO_2, N_2
32*	4.29×10^{-9}	O_2
44*	4.11×10^{-8}	CO_2
64.5*	2.79×10^{-9}	Xe

2.0 Calculate CO principal peak at mass 28. Cracking coefficients are obtained by interpolation of the data in Figures 3-6 and 3-7.

(i) Calculate CO_2 contribution at mass 12.

CO_2 (@ mass 12) = (CO_2 cracking coefficient at mass 12) * CO_2 (@ mass 44)

$= 0.053 * 4.11 \times 10^{-8} = 2.18 \times 10^{-9}$

(ii) Calculate CO contribution at mass 12.

CO (@ mass 12) = $3.02 \times 10^{-9} - 2.18 \times 10^{-9} = 8.42 \times 10^{-10}$

(iii) Calculate CO principal peak at mass 28.

CO (@ mass 28) = CO (@ mass 12)/ (CO cracking coefficient at mass 12)

$= 8.42 \times 10^{-10} / 0.036 = \underline{2.34 \times 10^{-8}}$

3.0 Calculate N_2 principal peak at mass 28. The CO contribution at mass 14 can be neglected as it is not significant.

N_2 (@ mass28) = N_2 (@ mass14) / (N_2 cracking coefficient at mass 14)

$= 4.92 \times 10^{-9} / 0.0801 = \underline{6.14 \times 10^{-8}}$

components were calculated using the peak separation procedure. Finally, calibration factors were applied to generate ratios between the principal peaks which matched the reference ratios (all partial pressures were normalized to the nitrogen partial pressure). Principal peak heights, the partial pressures and ratios of the reference mixture, and the calibration factors are summarized in Table 3-3. The calibration factors show a standard deviation of 4-8%.

Calibration for hydrogen was performed separately using a CO_2:H_2 gas mixture. The gases were allowed to equilibrate for two hours before being introduced into the laser. Principal peaks for CO_2 and H_2 were measured directly, and the calibration factor for hydrogen is shown in Table 3-3. Water vapor and xenon were not calibrated relative to the other gases thus only relative changes in their pressures could be accurately measured.

Table 3-3

Calibration Coefficients for CO_2, N_2, CO, O_2, and H_2

Gas	Reference Composition(1)	Analyzed Composition(1)	Calibration Factors
CO_2	1.00	1.00	1.00
N_2	0.998 ± 0.04%	1.052 ± 3.7%	0.949 ± 3.7%
CO	0.794 ± 0.04%	0.946 ± 7.6%	0.839 ± 7.6%
O_2	1.004 ± 0.04%	0.630 ± 6.8%	1.594 ± 6.8%
H_2 (2)	0.160 ± 3%	0.163 ± 5.3%	0.980 ± 8.3%

(1) Reference and analyzed composition values are relative to the partial pressure of CO_2.

(2) H_2 calibration was performed using a CO_2:H_2 gas mixture.

CHAPTER 4
LASER GAS CHEMISTRY EXPERIMENTS

A series of experiments, using the equipment and gas analysis techniques outlined in Chapter 3, were carried out to investigate those plasma chemical reactions which directly affect the lifetime of sealed CO_2 waveguide lasers. The majority of these experiments measured the effect of laser operating parameters on CO_2 dissociation. Other tests were conducted to measure the effects of water vapor and hydrogen on CO_2 dissociation and laser output power.

4.1 Experimental Procedures

All discharge experiments were carried out using the epoxy-sealed 5 watt laser described in Chapter 2. Prior to each test the laser was pumped and baked at 70°C for six hours and then pumped out at room temperature for 12 to 18 hours in order to maintain a constant background water vapor pressure of approximately 6×10^{-9} torr. Variations in water vapor levels were restricted to less than ±20% using this technique. Increases in background nitrogen and oxygen levels, indicative of air leaks, were also monitored. The laser was then filled with the desired gas mixture and the RGA chamber was pumped down to a base pressure of between 5×10^{-9} and 8×10^{-9} torr before gas sampling was started. The turnaround time between background analysis and the first gas sample was typically 3 to 4 hours.

Gas samples were removed from the laser at the back optical mount, as shown in Figure 2-2. The leak valve was connected to the laser by a six inch length of flexible stainless steel tubing. Detection of changes in laser gas

composition were thus limited by the diffusion time constant of gas molecules from the discharge region to the leak valve. A measurement was made of the diffusion time constant for CO_2 through a mixture of N_2 and He. A 3 cm^3 chamber containing 100 torr of CO_2 was attached to the auxiliary gas sampling port (see Figure 2-2) and isolated through a valve. The laser was evacuated, filled with 100 torr of a 3:1 He:N_2 gas mixture, and the valve was opened to allow the CO_2 to diffuse into the laser. The partial pressure of CO_2, measured as a function of time, is shown in Figure 4-1. The diffusion time constant, defined to be 95% of the time for the system to reach equilibrium, was slightly longer than 3 hours.

Several additional factors were considered in sampling from the laser discharge. Gas sampling was performed at a constant total pressure of $5x10^{-7}$ torr, rather than with a constant valve conductance, because it was not possible to repeatably set the gas sampling valve to a given conductance. As a result, pressure changes inside the laser caused by heating, increases in the amount of gas as a result of CO_2 dissociation, and pressure decreases as a result of gas sampling, caused apparent shifts in gas composition. Consider, as an example, a mixture of 50 torr of CO_2 and 50 torr of N_2. If there was 50% CO_2 dissociation the total pressure would rise to 112.5 torr and the percentage nitrogen composition would fall to 44.4%. To counter this problem all measurements were normalized to a constant xenon pressure, as xenon has not been reported to participate in any significant chemical reactions. Although gas sampling will gradually change the gas composition because of the mass dependence of conductance, this effect is not significant and was ignored.

In all tests where laser output power was recorded, the optics were readjusted for maximum single-mode output power at each measurement. Gas

Figure 4-1

Measurement of the Diffusion Time Constant for CO_2 through a 3:1 $He:N_2$ Gas Mixture

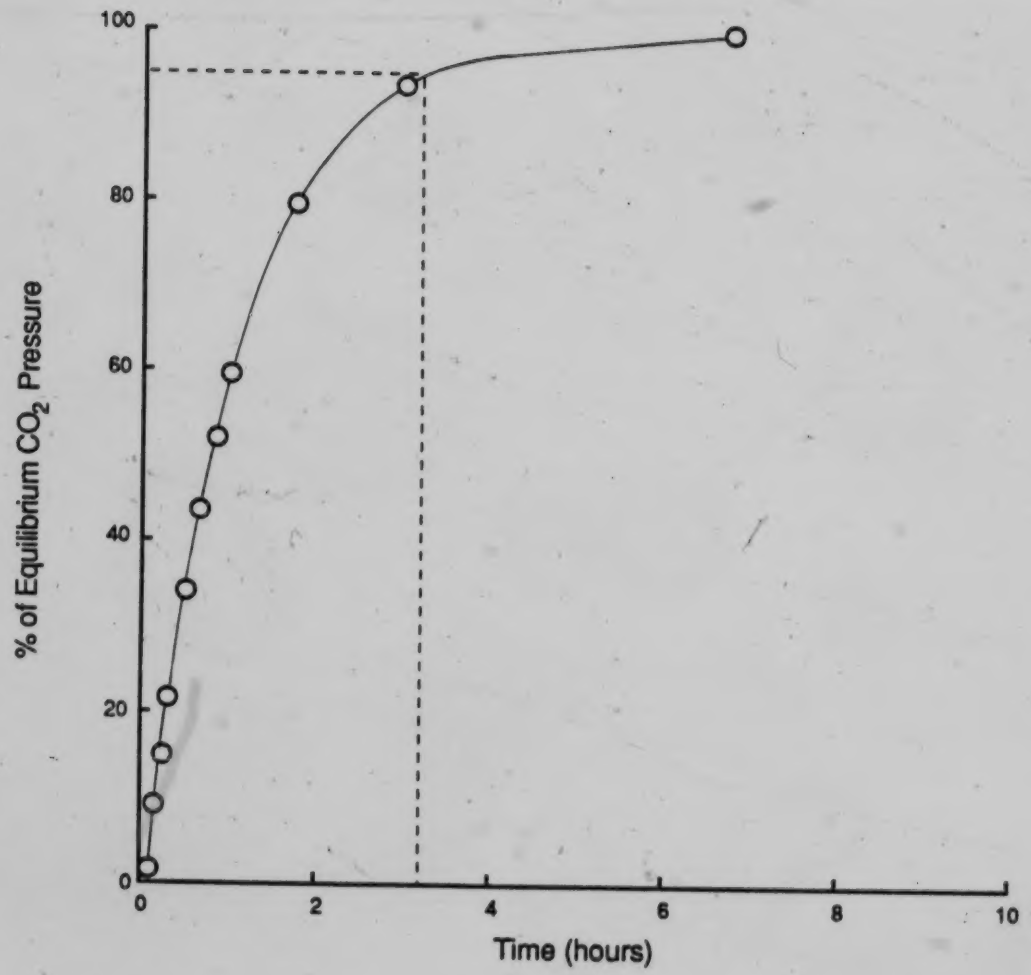

analyses were made using the calibration factors and cracking patterns calculated in Chapter 3.

4.2 Preliminary Measurements

A preliminary set of measurements with the objective of observing general trends in short-term gas composition was first completed. A representative test of 68 hours duration will be discussed in more detail. The laser was filled with 80 torr of a mixture of 11.9% CO_2, 11.9% N_2, 71.2% He, and 5.0% Xe (this mixture was found to give peak output power by Sinclair[64] and was subsequently used as the standard mixture for all tests) and the test was conducted at an RF input power level of 40 watts. The partial pressures of CO_2, CO, N_2, O_2, H_2O, and H_2 were measured using the analysis technique of Chapter 3. As shown in Figure 4-2, laser output power rose from 2.7W to 3.35W over the first 9 hours, remained constant over the next 20 hours, and fell to 2.7W by the end of the test. Time variations in the CO_2 partial pressure and in the CO/O_2 partial pressures are shown in Figures 4-2 and 4-3 respectively.

CO_2 levels fell to 39.5% of their starting value within 4 hours and then rose throughout the remainder of the test to a final value of 79%. Water vapor, which is known to significantly reduce CO_2 dissociation levels, was believed to be responsible for the decrease in CO_2 dissociation observed after the first 4 hours of the test. The minimum CO_2 level is much higher than reports of 10-15% dissociation by Laakmann[8,20], but very close to the 72% dissociation observed by Williams and Smith[22] under similar discharge conditions (30W input power; 75 torr of a 13% CO_2, 9% N_2, and 78% He mixture). The four hour time taken to reach a minimum CO_2 level is very close to the diffusion time constant for CO_2. Visual observation of the time taken for the discharge color to change from pink to white (the discharge bleaches to white as the CO and O_2 pressures build

Figure 4-2

Preliminary Lifetime Test
Laser Ouput Power and CO_2 Partial Pressure vs Time

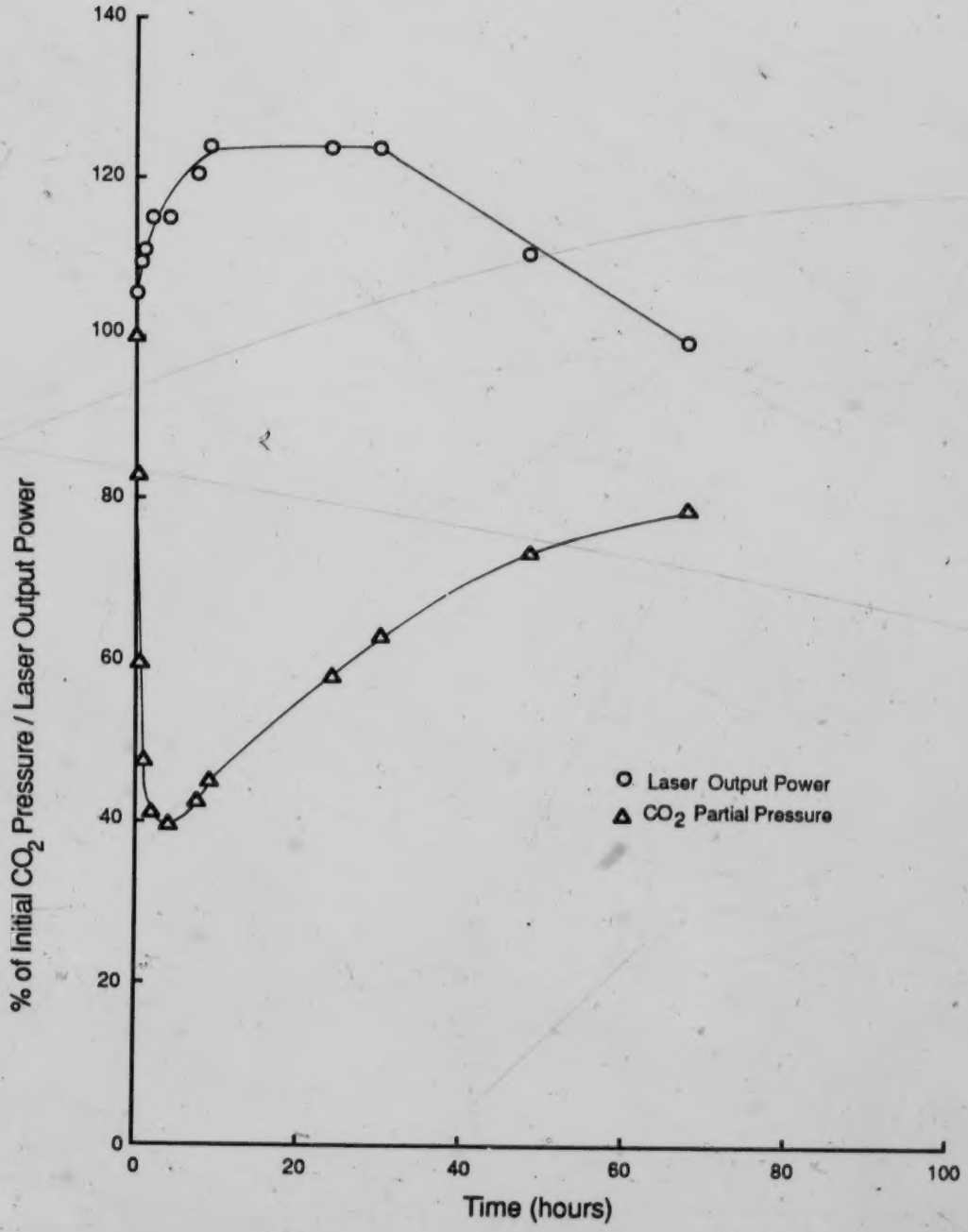

Figure 4-3

Preliminary Lifetime Test
CO and O_2 Partial Pressure vs Time

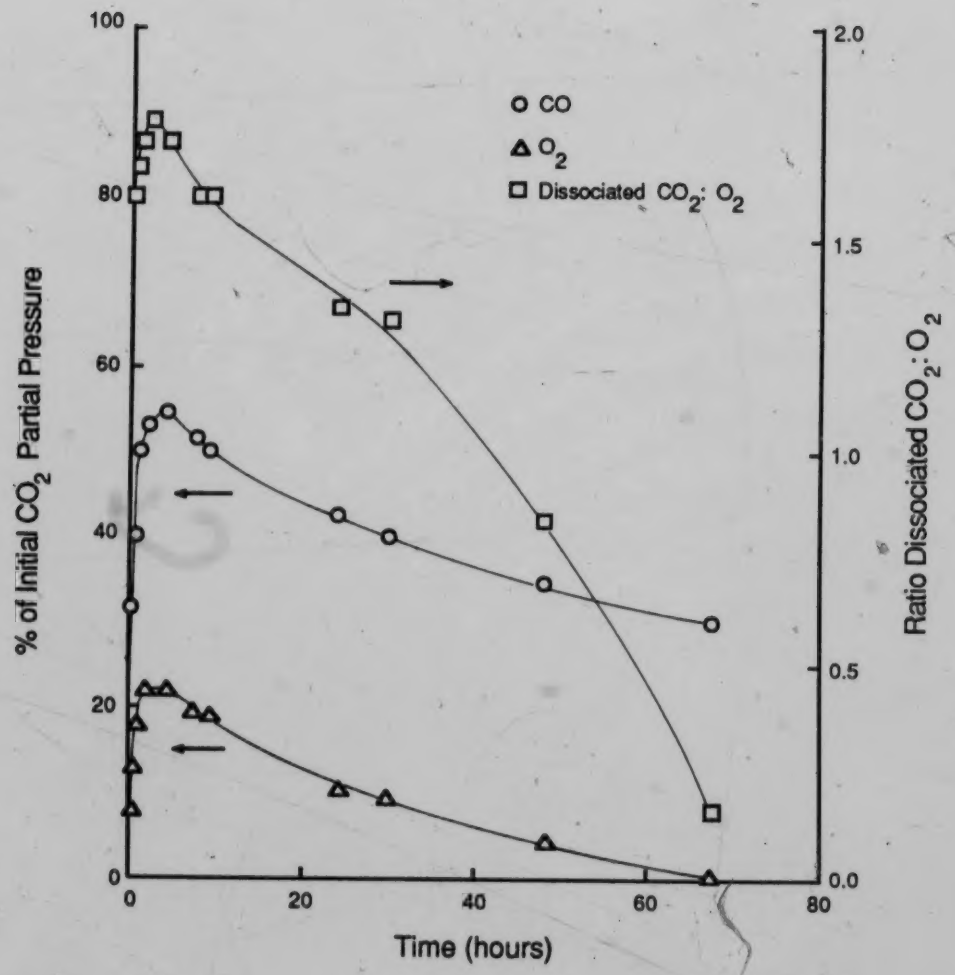

up[54]) indicated that significant CO_2 dissociation occurs in the discharge region within the first 10 seconds after turn-on.

Oxygen loss is clearly evident in Figure 4-3. Although significant quantities of oxygen were produced during the first 10 hours of the test as a result of CO_2 dissociation, there was almost no oxygen remaining in the laser at the end of 68 hours even though the CO_2 level had risen to only 80% of its initial value. The effect is seen more clearly by considering the ratic of dissociated CO_2 to measured O_2, also shown in Figure 4-3. Theoretically, given the dissociation reaction $CO_2 \rightarrow CO + 1/2O_2$, this ratio should have been 2.0. Over the short term, ratios of 1.6 to 1.8 were observed (the discrepancy between measured and theoretical values is attributed to errors in calibration for oxygen) however for times exceeding 24 hours the ratio fell rapidly until a value of 0.08 was recorded at the completion of the test. Oxygen is likely being adsorbed on laser tube surfaces but the exact mechanism for this process is unknown. The loss of oxygen did not appear to have any effect on CO_2 recombination.

The water vapor partial pressure (see Figure 4-4) showed a sharp initial rise in the first 2 hours of the test followed by a linear rate of increase indicative of outgassing. This can be compared with the outgassing rate for water vapor measured at room temperature (20°C) which was lower by 29%. Water vapor could also have been produced by the reaction of outgassed hydrogen and oxygen released by CO_2 dissociation. This mechanism should have produced noticeable nonlinearities in the water vapor pressure (because both the hydrogen and oxygen partial pressures were highly nonlinear with respect to time) which were not observed.

Figure 4-4

Preliminary Lifetime Test
Water vapor and Hydrogen Pressure vs Time

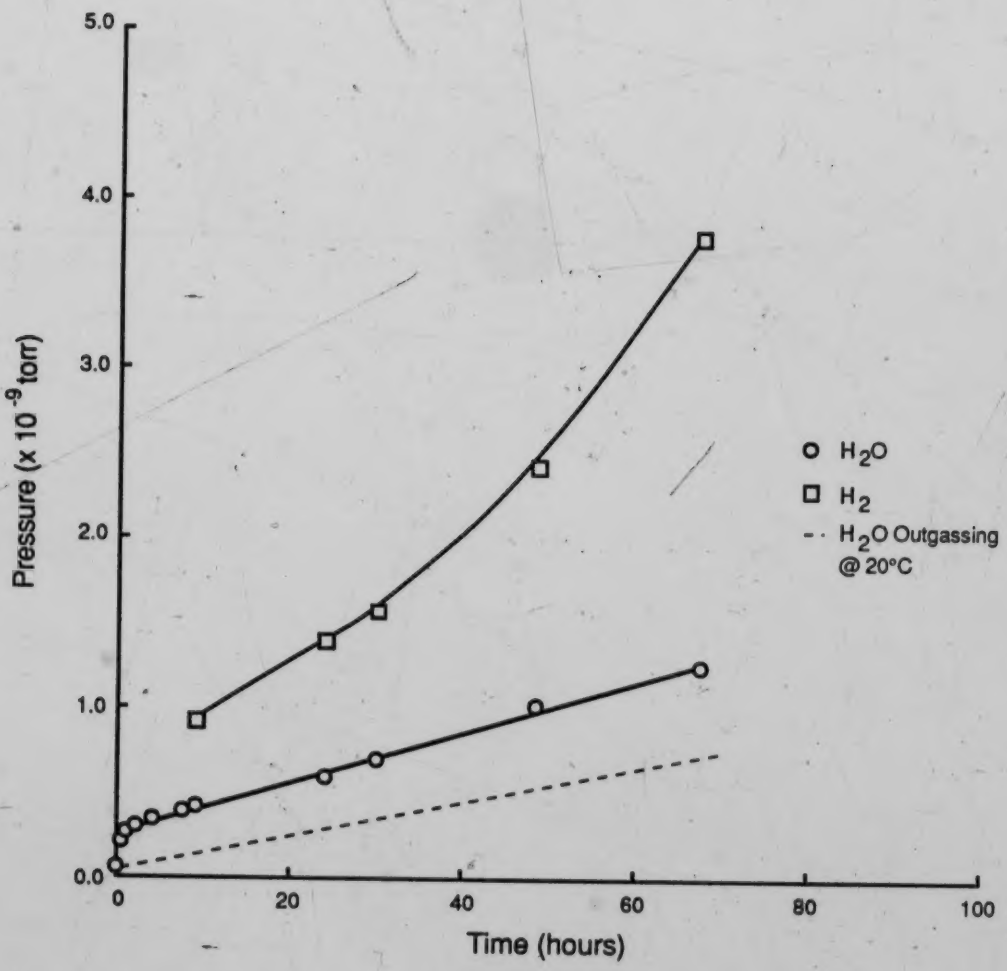

Hydrogen could not be measured over the first 10 hours of the test as it was obscured by the large helium peak at mass 4. The only known source of hydrogen is outgassing from laser tube surfaces. The hydrogen partial pressure rose continuously but nonlinearly as shown in Figure 4-4.

The increase in output power observed over the first few hours of operation is attributed to the more efficient excitation of the 00^01 level of CO_2 by collisional energy transfer from excited CO[65]. The drop in output power is attributed to the build up of water vapor and hydrogen in the discharge. As discussed in Chapter 1, water vapor and/or hydrogen have been shown to be the primary cause of power degradation in sealed waveguide lasers. These were the only gases whose concentration was observed to rise continuously over the duration of the test. Water vapor[66] and hydrogen concentrations of 0.12% and 0.3% were present when the first power decrease was observed.

The presence of the oxides of nitrogen, NO and NO_2, which are known to seriously degrade the performance of sealed DC-excited lasers[67] at concentrations of less than 0.1%, was monitored at mass peak 30 (the NO_2 principal peak at mass 46 would have been obscured by a secondary CO_2 peak). No increase in the level of this peak was detectable. To date, reports of nitrogen oxides in RF-excited CO_2 waveguide lasers have all been negative. However Williams and Smith[22] measured up to 20000 ppm of NO when directly sampling a RF-excited CO_2:N_2:He flowing-gas discharge through a differentially-pumped 100μ pinhole. Levels of NO dropped to 200 ppm when gas sampling was moved to the discharge afterglow. The failure to detect nitrogen oxides from working lasers may thus be related to gas sampling techniques.

These preliminary experiments demonstrated many of the important phenomena investigated in greater detail in the following sections. These include: CO_2 dissociation and recombination, oxygen consumption, and an approximate laser lifetime of 100 hours. It is believed that both the decreases in laser output power and the equilibrium CO_2 dissociation levels are strongly dependent on water vapor and/or hydrogen concentration.

4.3 CO_2 Dissociation Measurements

A series of tests were made to determine the effects of pressure, gas mixture, and RF input power on CO_2 dissociation levels. The effect of H_2O and H_2 on CO_2 dissociation and laser output power are considered separately in section 4.4. The objectives of these tests were twofold. The first was to identify a combination of operating parameters which will minimize CO_2 dissociation. This should prolong laser lifetime by reducing the influence of oxygen absorption. Oxygen absorption was observed in preliminary tests and is a relatively difficult problem to solve as it is often related to a specific material or processing step. For example Laakmann[28] traced oxygen absorption in their lasers to nickel coatings on aluminum parts and were forced to introduce a nitric acid passivation step into their laser processing procedures.

A second objective of these experiments was to extend and corroborate existing dissociation measurements of RF-excited CO_2 waveguide laser discharges. A set of experiments by Williams and Smith[22] provides the most comprehensive source of data at this time. Most of these measurements were, however, performed under flowing gas conditions in large-bore glass discharge tubes. Discharge scaling laws were then used to infer comparable results for

laser waveguides. Smith admits that measurements obtained under these conditions do not accurately model the wall effects in small-bore waveguides.

Measurements of CO_2 dissociation as a function of pressure were performed at 50, 65, 80, 120, and 140 torr using gas mixtures of 11.9% CO_2, 11.9% N_2, 71.2% He, and 5.0% Xe at an RF input power of 40 watts. The variation in CO_2 partial pressure with time was as shown in Figure 4-5. In all cases an equilibrium was reached after 2 to 4 hours and dissociation levels fell again soon afterward (this was attributed to the effects of water vapor). Dissociation increased with pressure, ranging between 53 and 71%. For a constant input power per unit volume, CO_2 dissociation should be proportional to pressure^{-1}[22]. As shown in Figure 4-6, there is good agreement between the experimental data points and the theoretical dependence. Clearly, however, pressure effects alone will not be sufficient to reduce CO_2 dissociation to less than 50%.

A series of measurements were then conducted to determine the effects of varying the proportions of helium and xenon on CO_2 dissociation. Both sets of measurements were carried out at a total pressure of 120 torr and an RF input power of 40W. As shown in Figures 4-7 and 4-8 CO_2 dissociation increases as the helium content in the gas mixture increases and decreases as the xenon content increases. These results are attributed to the effects which both of these gases have on the electron energy distribution in CO_2 discharges. Helium-rich mixtures contain more high-energy 7eV electrons while xenon, with a large momentum transfer cross-section which peaks at an energy of 9 eV, greatly reduces the number of high-energy electrons in the discharge. Xenon levels in excess of 5% are not expected to result in further significant decreases in CO_2 dissociation. Measurements of the reduction in electron temperature with the

Figure 4-5

CO_2 Partial Pressure vs Time as a Function of Pressure

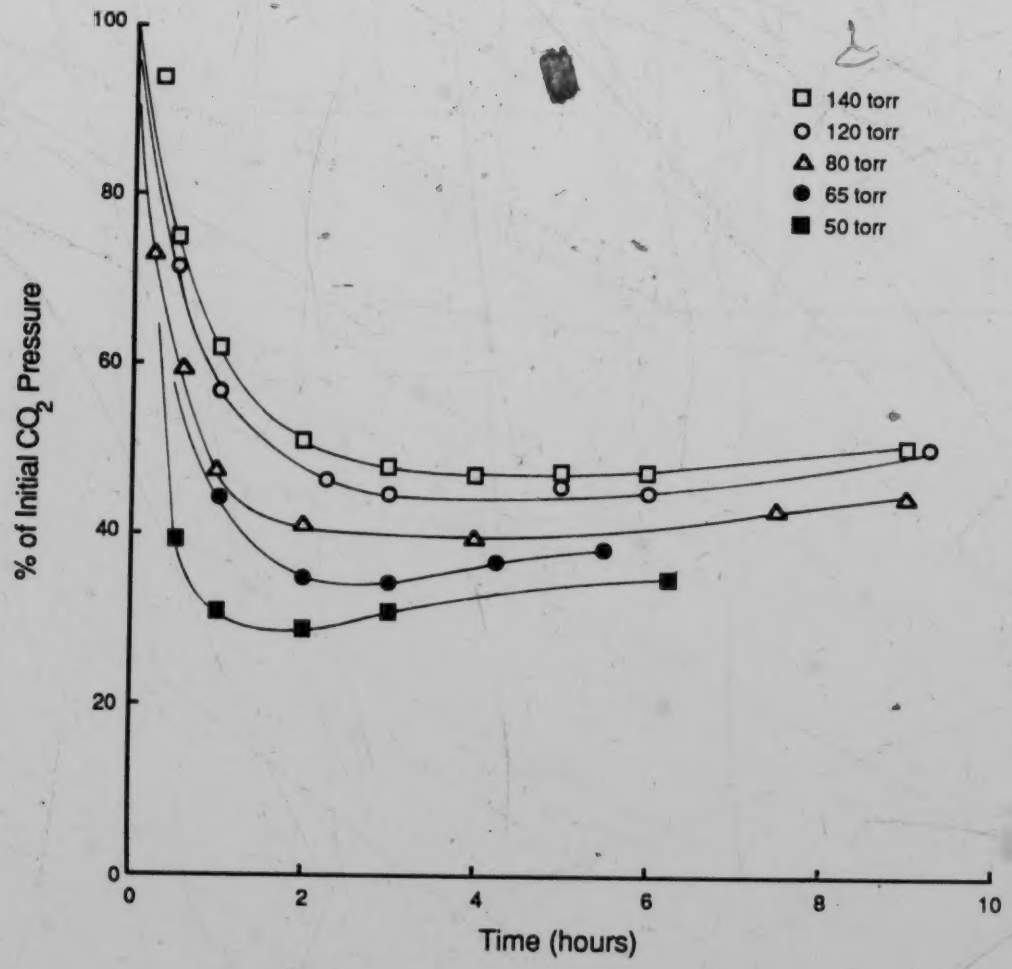

Figure 4-6

CO_2 Dissociation vs Pressure^{-1}

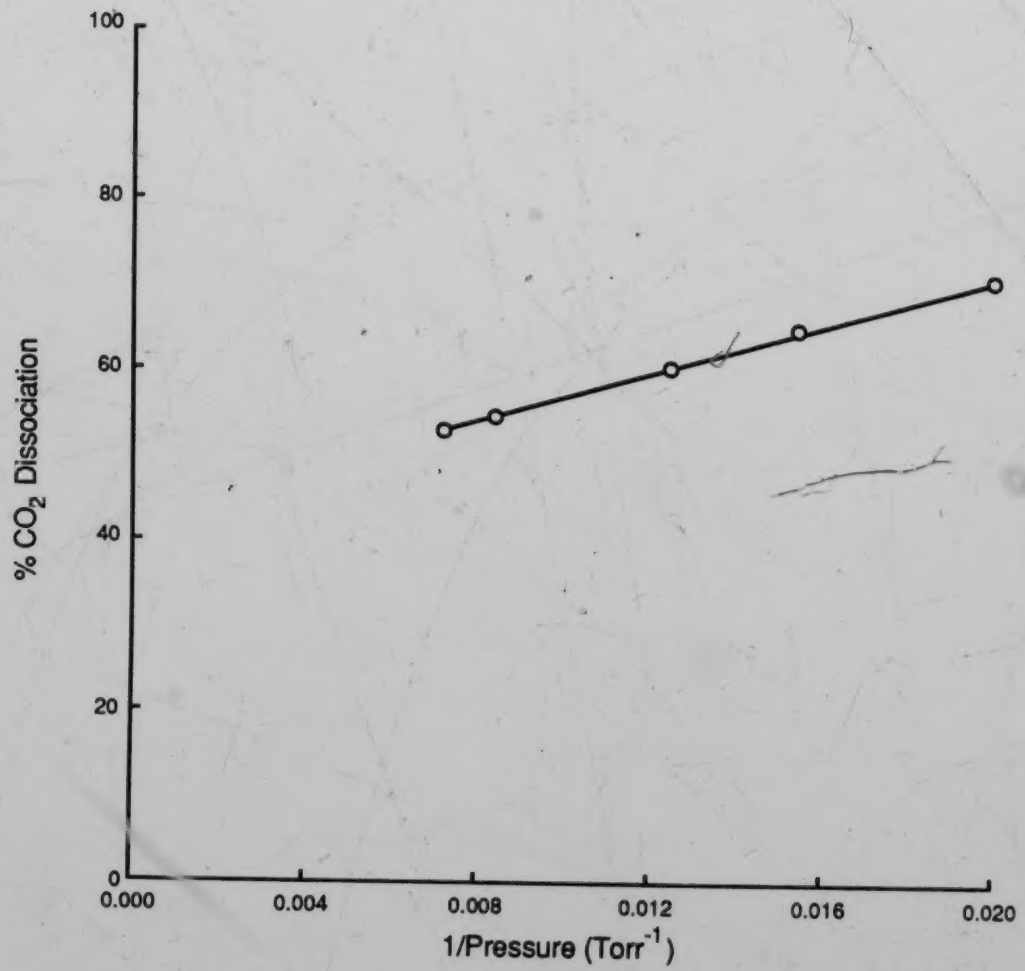

Figure 4-7

CO_2 Partial Pressure vs Time as a Function of He Content

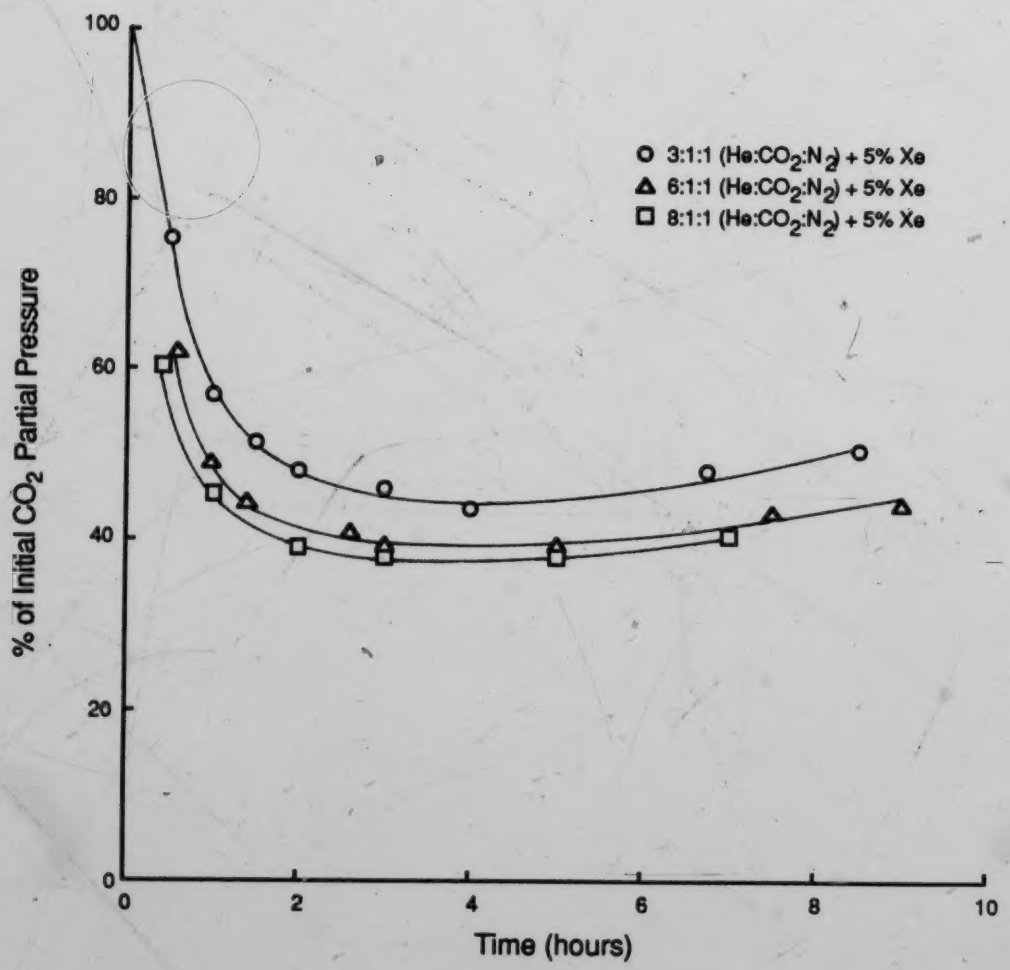

Figure 4-8

CO_2 Partial Pressure vs Time as a Function of Xe Content

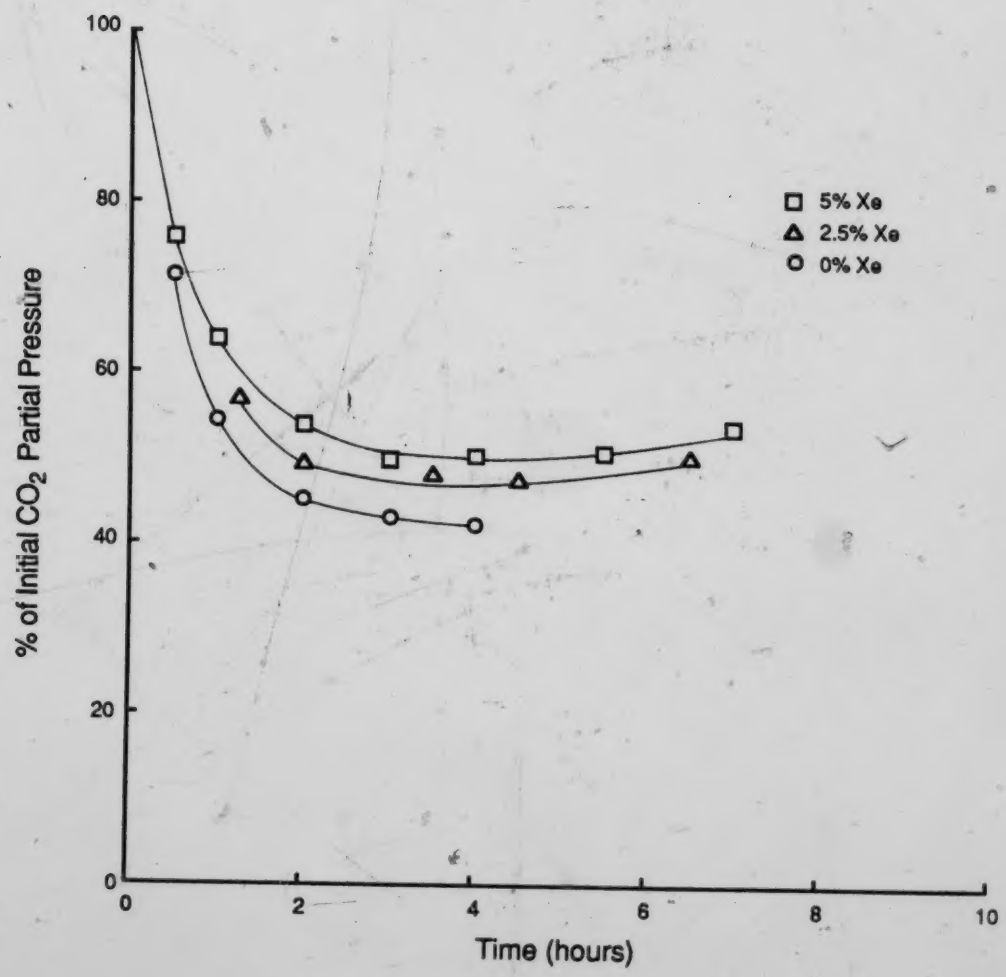

addition of xenon[68] show little additional effect when xenon levels exceed a few percent. Variations in helium and xenon content thus had a relatively minor effect on CO_2 dissociation, causing a maximum shift in the equilibrium dissociation levels of about ±10%.

Discharge tests were performed at four input power levels: 40, 50, 60, and 70 watts, or expressed as power per unit length: 2.7, 3.3, 4.0, and 4.7 watts/cm. These power levels range from 40% to 70% of the input power required to produce 40W of output power from a 60 cm laser currently under construction. Input power levels in the 15 cm laser were limited to 70W by differential thermal expansion between the ceramic waveguide, the epoxy, and the stainless steel optical mounts. All tests were performed with a mixture of 11.9% CO_2, 11.9% N_2, 71.2% He, and 5.0% Xe at a pressure of 120 torr. As shown in Figure 4-9, CO_2 dissociation levels are virtually identical at each of the four power levels. This effect is attributed to the relative invariance of the discharge electric field to pressure ratio, E/P, with input power. The CO_2 dissociation rate constant for electron impact dissociation is known to be strongly tied to E/P. Measurements of E/P in 80 torr of a He:CO_2:N_2 mixture by Griffith[31] show only a 12% variation over an RF input power range of 10 to 70W. Oxygen and water vapor levels were also examined to determine to what extent RF input power influences oxygen absorption and water vapor outgassing. As shown in Figures 4-10 and 4-11 there was not a well defined difference in the rate of oxygen absorption but there was a 180% increase in the rate of water vapor outgassing as the power levels increased from 40 to 70W. The most important lifetime effect of increasing the input power levels will thus be to increase water vapor outgassing rates and the consequent deterioration in laser output power. Laakmann[8] have used this effect for accelerated lifetime

Figure 4-9

CO_2 Partial Pressure vs Time as a Function of RF Input Power

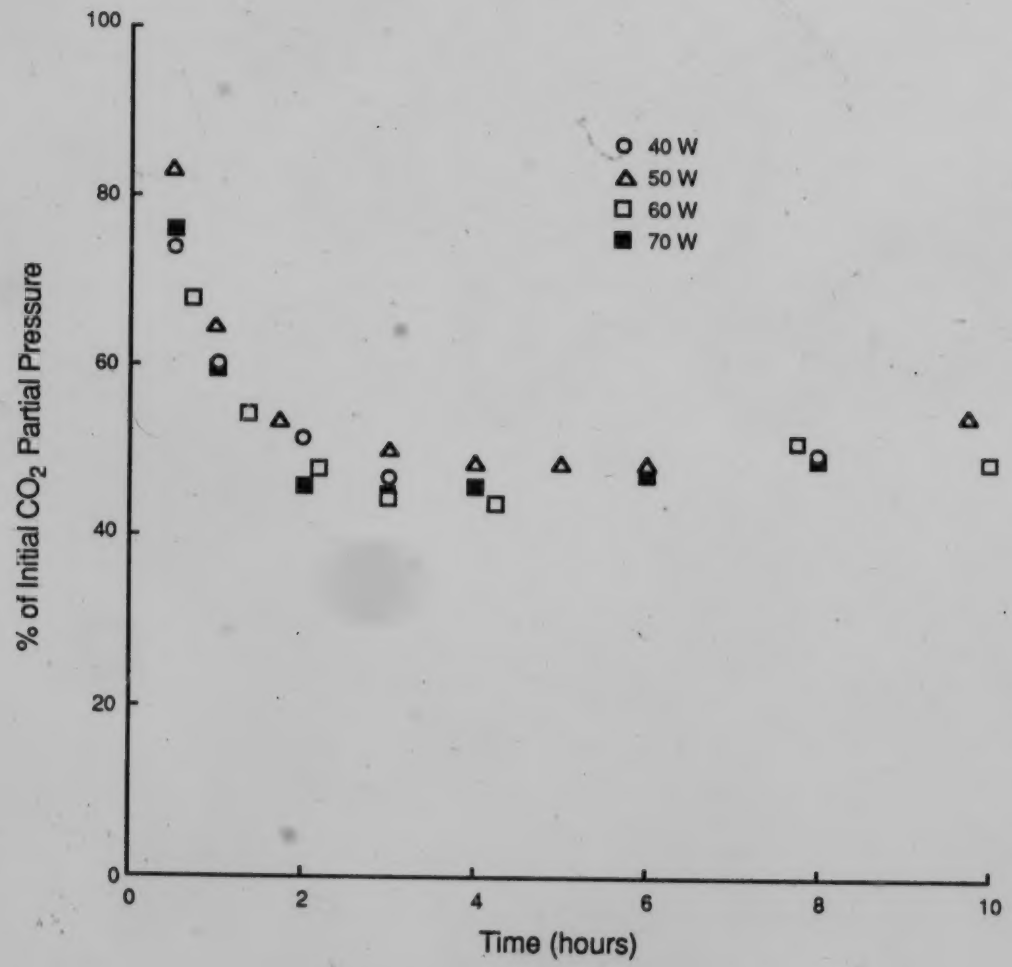

Figure 4-10

O_2 Partial Pressure vs Time as a Function of RF Input Power

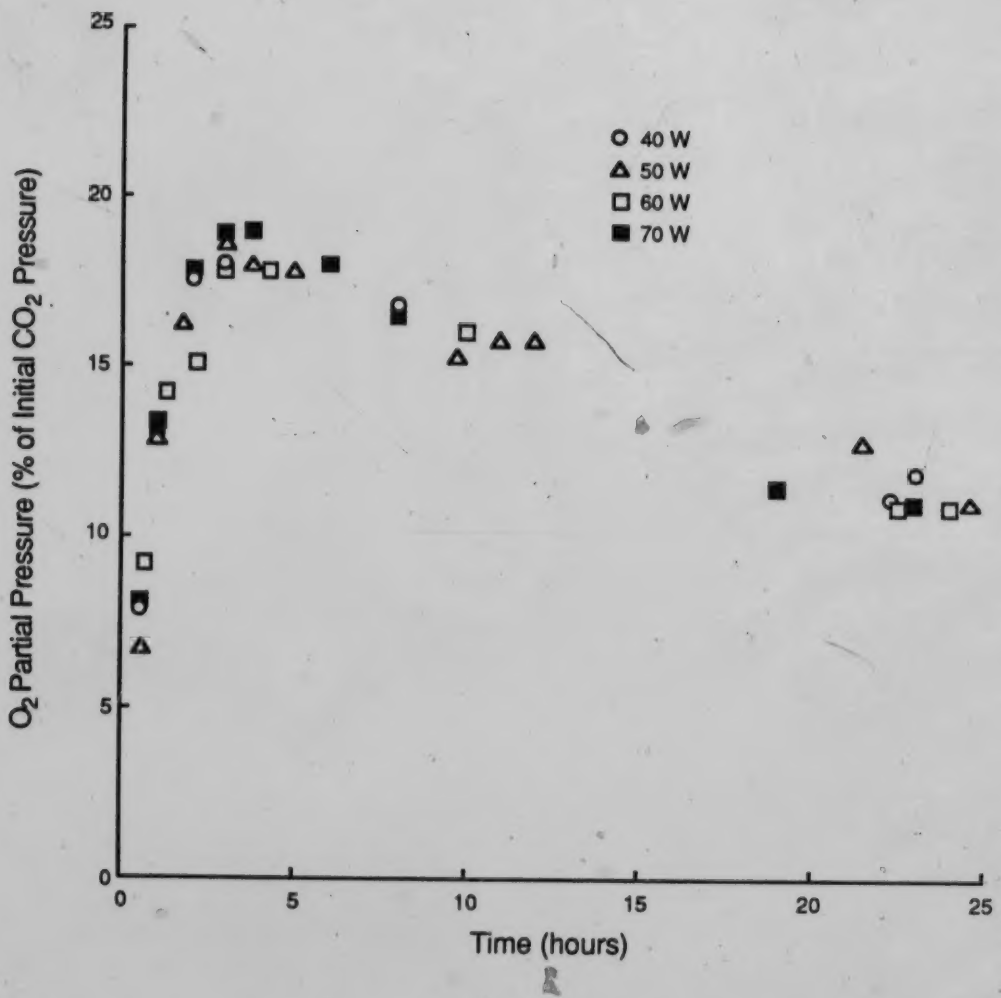

Figure 4-11

H_2O Partial Pressure vs Time as a Function of RF Input Power

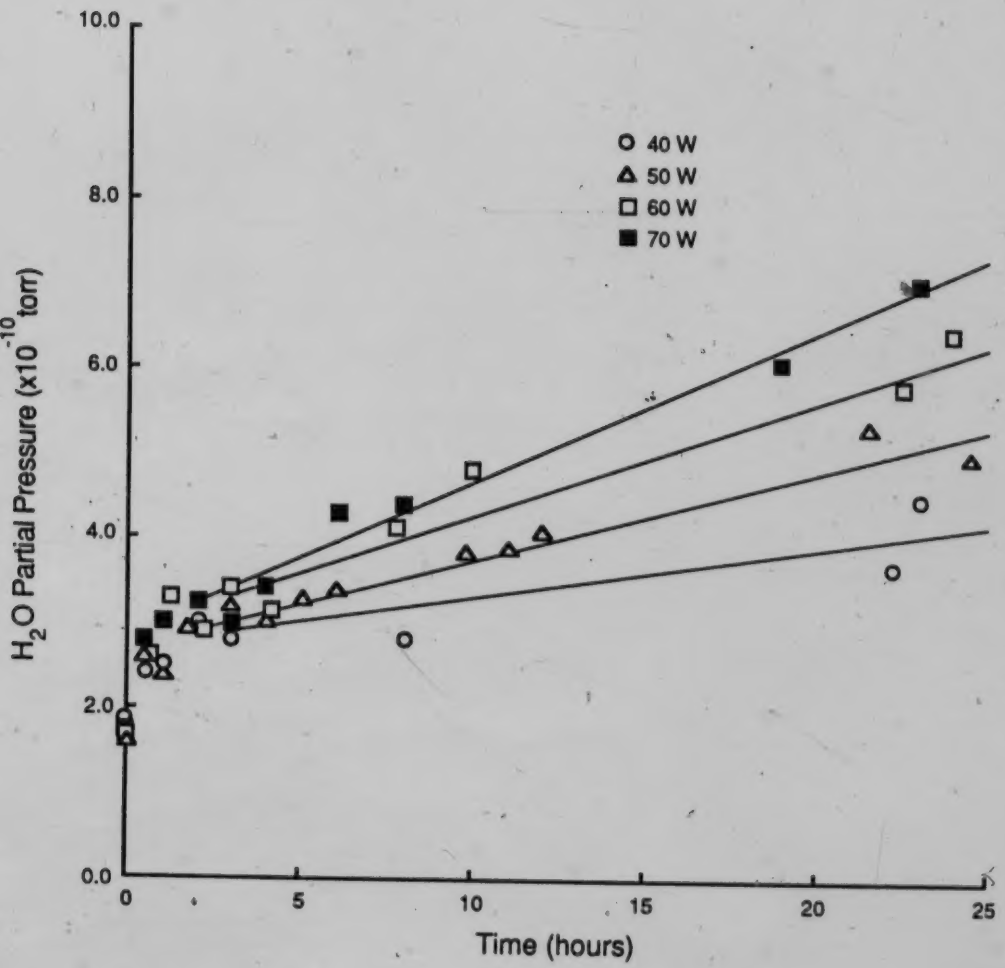

testing of their lasers. Lasers which operated for 500 hours at 20°C were found to fail after 5 hours at 100°C.

4.4 Hydrogen and Water Vapor Measurements

As discussed in Chapter 1, output power degradation in sealed CO_2 waveguide lasers has been largely attributed to the build-up of hydrogen and/or water vapor in the discharge. Hydrogen and water vapor are also responsible for the reformation of CO_2 as a result of the reaction

$$OH + CO \longrightarrow CO_2 + H.$$

Preliminary examination of laser gas chemistry in section 4.2 resulted in data which can be explained by the presence of water vapor and hydrogen in the discharge. Laser output power and CO_2 dissociation were both observed to decrease as the water vapor content in the discharge increased. A number of discharge tests were thus conducted to more closely examine the effects of water vapor and hydrogen in sealed CO_2 waveguide lasers. The three following gas mixtures were used:

(i) 120 torr of 11.9% CO_2, 11.9% N_2, 71.2% He, 5% Xe, and 0.02% H_2O. (This was the normal level of water vapor observed following the standard pumping and baking procedures).

(ii) Identical to (i) except the water vapor content was increased to 0.10% by eliminating bake-out.

(iii) 120 torr of 11.9% CO_2, 11.9% N_2, 69.2% He, 5% Xe, 2% H_2, and 0.12% H_2O. (The hydrogen was contaminated with water vapor).

All tests were conducted with an RF input power of 40W.

As discussed in section 4.1 the gas analyzer was not calibrated for water vapor. Estimated water vapor concentrations were calculated by taking into account the conductance and ionization efficiency of water vapor relative to nitrogen.

A comparison of the results of the discharge tests using gas mixtures containing 0.02% and 0.10% water vapor demonstrates clearly that water vapor is responsible for decreased output power. As shown in Figure 4-12, in the gas mixture with low water vapor levels output power remained essentially constant at 2.65W. (This is in contrast to earlier measurements, performed under similar conditions, in which laser output power was observed to rise from 10 to 20% over starting values during the first 5 to 10 hours of operation. The lower output power is attributed to an increase in cavity losses caused by the onset of optical damage. Output power was also observed to drop from 0 to 5% over the first 5 to 10 hours of operation when the laser was operated under low-gain conditions, such as with gas mixtures lacking xenon.) In the gas mixture with added water vapor the turn-on power was lower at 2.5W, and dropped continuously over the five hour duration of the test to a final value of 1.7W. Hydrogen is not believed to have affected output power in these measurements. Hydrogen levels during both tests were below those in preliminary measurements (see Figure 4-4) where no drop in output power was observed. Laser output power is presented as a function of water vapor concentration in Figure 4-13. The threshold level for water vapor was approximately 0.1%. This figure was substantiated by the examination of water vapor levels in all discharge tests exceeding 20 hours.

Discharge tests using the gas mixture containing H_2 showed that hydrogen concentrations of 2% are capable of suppressing laser action. As

Figure 4-12

Water Vapor Test
Laser Ouput Power and Water Vapor Concentration vs Time

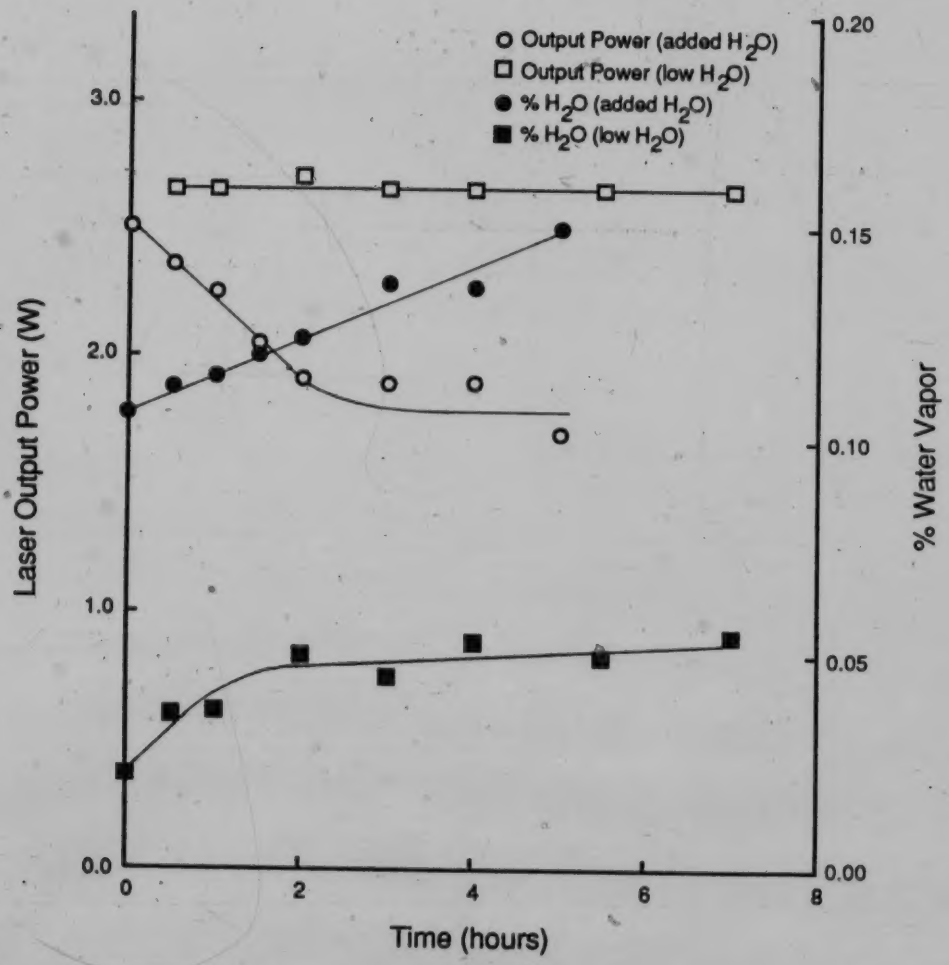

Figure 4-13

Laser Output Power vs Water Vapor Concentration

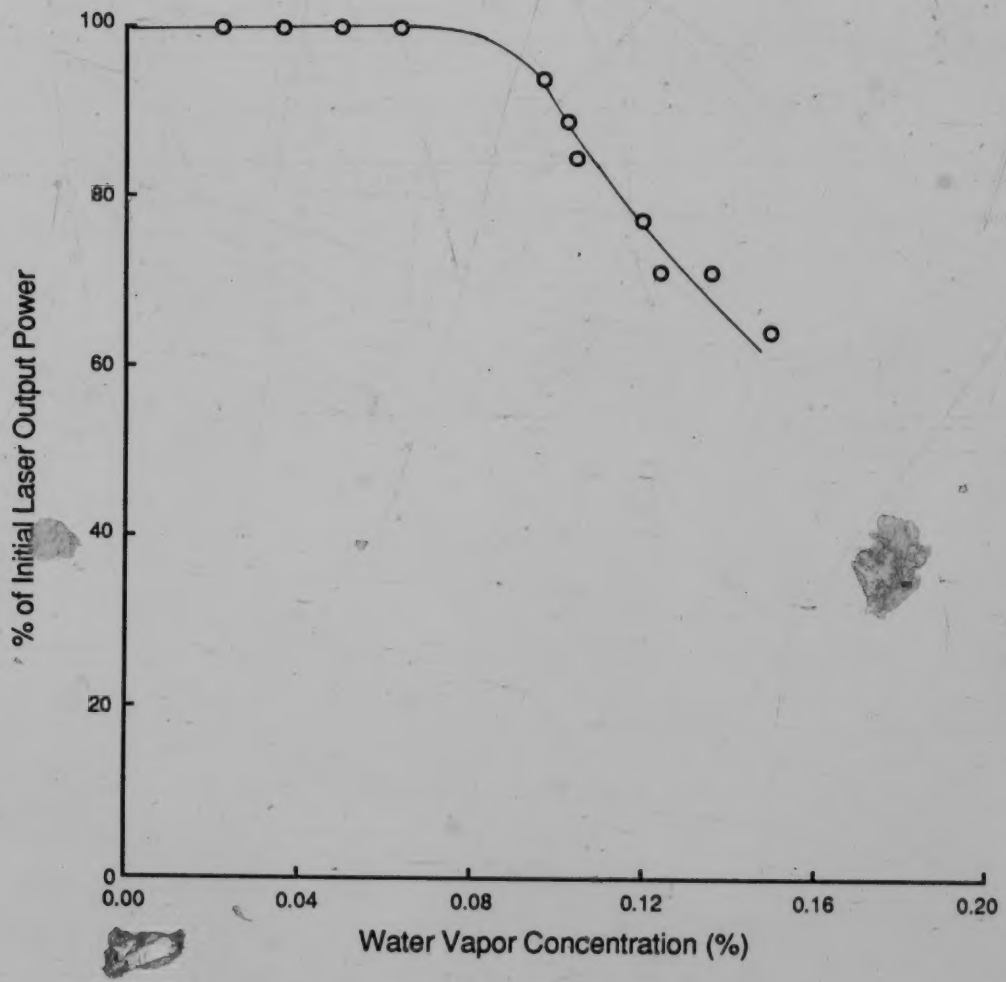

Figure 4-14

Hydrogen Test
Laser Ouput Power and Hydrogen and
Water Vapor Concentrations vs Time

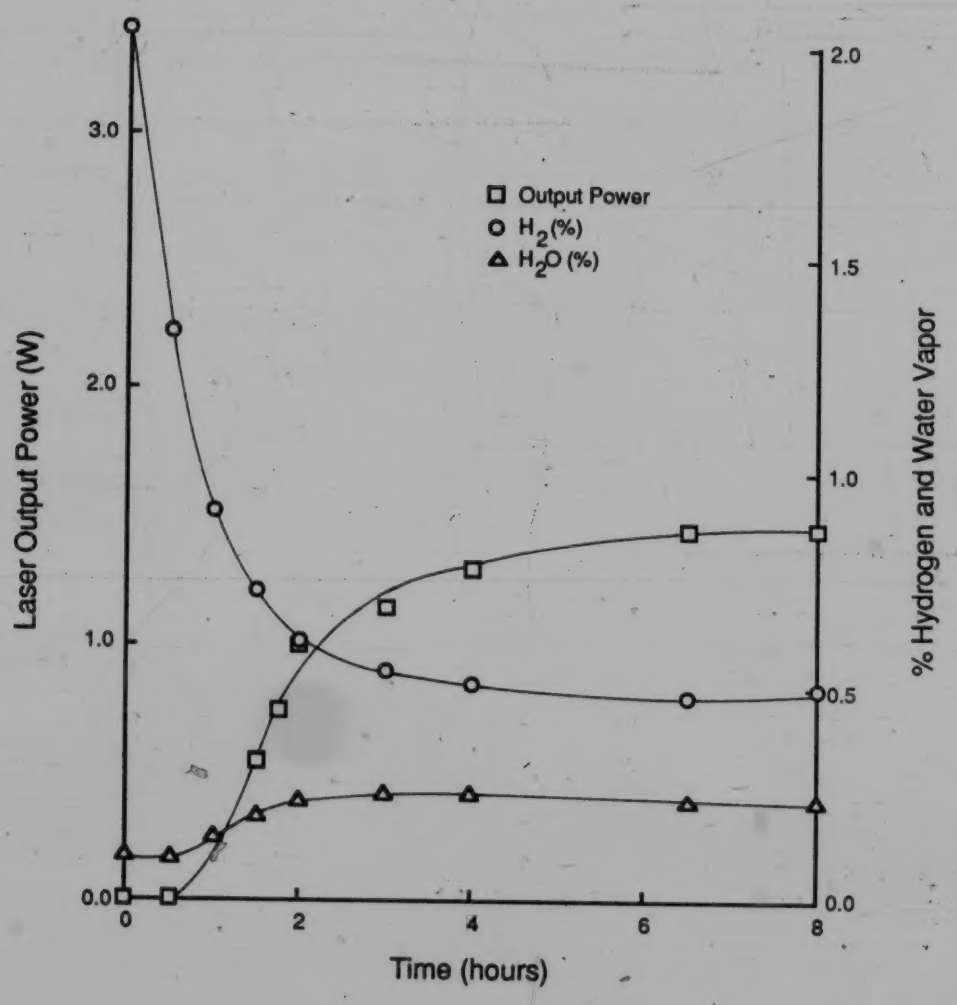

Figure 4-15

Laser Output Power vs Hydrogen Concentration

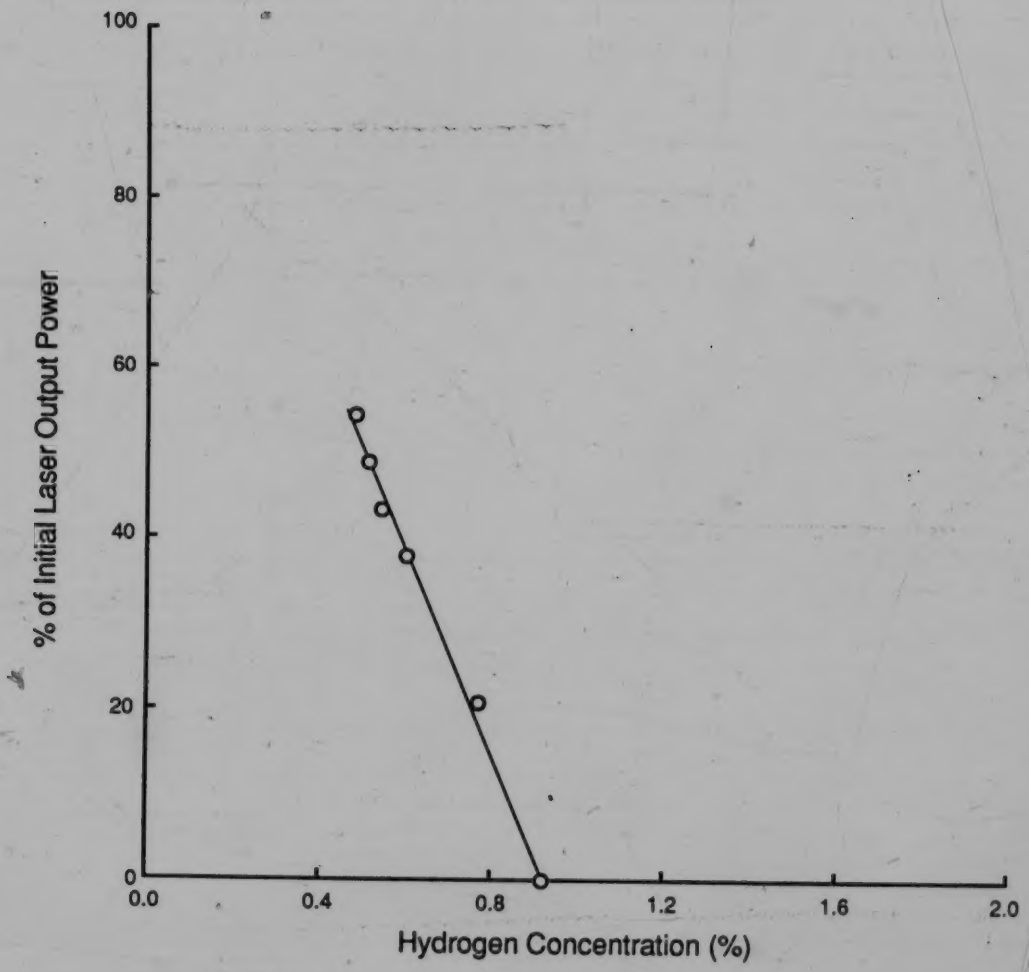

Figure 4-16

CO_2 and O_2 Partial Pressures as a
Function of Hydrogen and Water Vapor Content

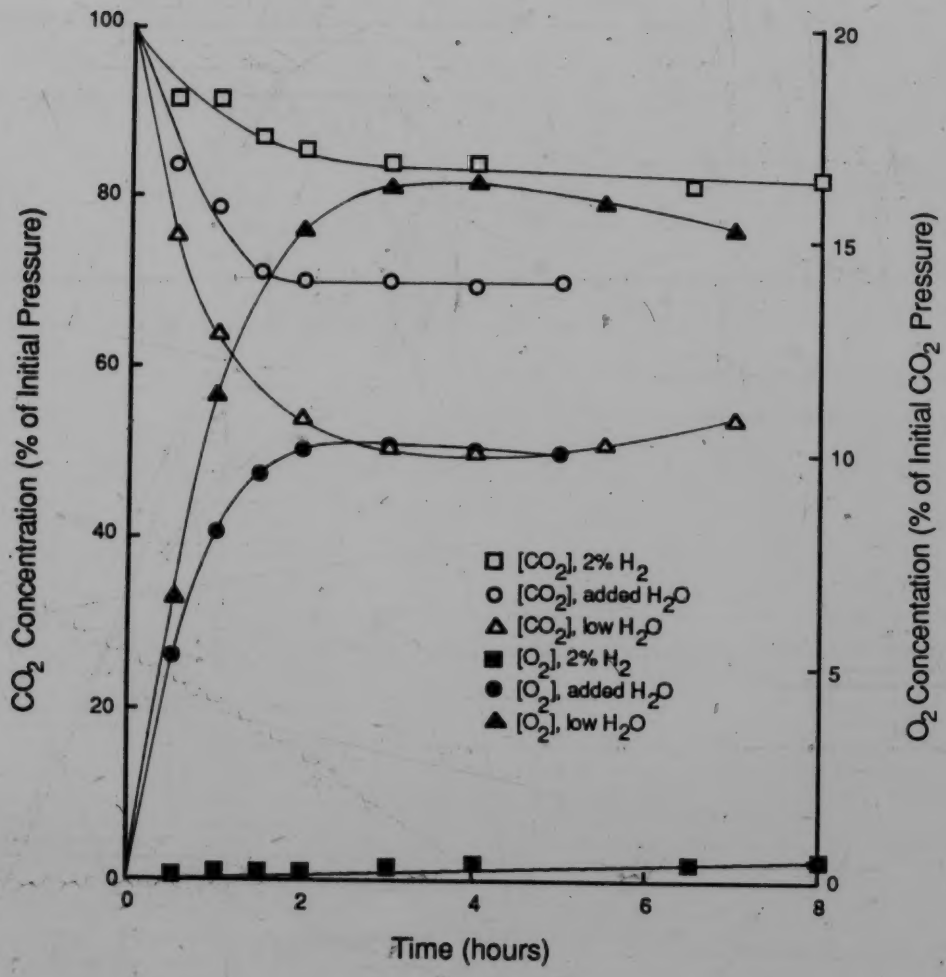

shown in Figure 4-14 hydrogen levels decreased rapidly after turn-on (probably as a result of reactions between hydrogen and oxygen which form water vapor) and output power was subsequently observed to rise to a maximum value of 1.45W. Power was first observed at a hydrogen concentration of 0.75%. Output power is presented as a function of hydrogen concentration in Figure 4-15. This does not account for the effects of water vapor whose concentration was as high as 0.25%.

The three gas mixtures also demonstrated clearly that CO_2 dissociation levels are controlled by the presence of hydrogen and water vapor in the discharge. As shown in Figure 4-16 dissociation levels dropped from 50% in the low water vapor gas mixture to 17.5% in the mixture containing hydrogen. The threshold level where water vapor begins to affect CO_2 dissociation was 0.06±0.01%. This figure was calculated by tabulating the water vapor levels in all discharge tests in which the reformation of CO_2 was observed.

4.5 Optical Damage

Over the duration of the gas chemistry experiments (a total time of 350 hours) the maximum output power of the laser, as measured with a fresh gas charge, was observed to decrease by approximately 40%. This decrease was attributed to optical damage as no other sources of degradation, such as vacuum leaks, were found. Examination of the optics revealed no particulate damage; however, there was noticeable discoloration, especially in areas directly adjacent to the ends of the waveguide. Under magnification, the surface deposits were observed to have an even but granular appearance. The bulk of the deposits were removed with methanol and gentle scrubbing and the residue had a reddish-brown color. The deposits could be the result of molecular

complexes which break up on collision with the surface of the optics or waveguide walls. This effect has been observed in conjunction with cathode sputtering in DC-excited CO_2 lasers[18] and the formation of beryllium carbonate deposits on the optics of an RF/DC-excited waveguide laser[69].

CHAPTER 5

CONCLUSIONS AND RECOMMENDATIONS

This thesis has involved the design and construction of sealed RF-excited waveguide CO_2 lasers and a high-vacuum laser processing station, as well as the study of the gas chemistry in RF-excited CO_2 waveguide laser gas mixtures. This chapter summarizes the results of these studies and presents a number of recommendations for future work.

Chapter 1 presented a summary of what is currently known about the lifetime-limiting factors in RF-excited CO_2 waveguide lasers and compared the lifetime implications of DC and RF excitation. Chapter 2 examined the factors involved in the design of sealed waveguide CO_2 lasers. The most important of these were shown to be materials, sealing techniques, and laser tube processing. An epoxy-sealed 5 watt laser, used in laser gas chemistry experiments, was constructed, and two prototype hard-sealed lasers were designed.

Chapter 3 presented four measurement techniques which have been used for the analysis of sealed CO_2 laser gas mixtures. Mass spectroscopy was selected and a high-vacuum laser processing station with an on-line residual gas analyzer was designed and constructed.

Chapter 4 summarized the results of gas chemistry experiments in sealed RF-excited CO_2 waveguide laser gas mixtures. Recorded lifetimes were limited to less than 100 hours by the build-up of outgassed water vapor and hydrogen in the discharge. A direct correlation was observed between increases in water vapor and hydrogen levels and decreases in laser output

power. Water vapor levels of approximately 0.1% were found to first affect laser output power.

The remaining experiments concerned the effect of discharge parameters on CO_2 dissociation. Hydrogen and water vapor, well known for their catalytic effect on CO_2 reformation, were found to significantly reduce CO_2 dissociation levels. This benefit was of course offset by their effect on laser output power. Dissociation levels were also reduced by increased pressure, decreased helium content, and increased xenon content. None of these factors were capable (within the normally allowed range of operating parameters) of reducing dissociation to less than 40%, which is considerably higher than previouly published data. Input power did not have a direct effect on dissociation, but it did increase the water vapor outgassing rate.

The work outlined in this thesis has resulted in significant contributions in two separate areas. First , a set of guidelines for the design and processing of sealed CO_2 waveguide lasers was established. The information, much of which would be considered proprietary by commercial laser manufacturers and is not available from any single source in the open literature, is a synthesis of experimental data, high-vacuum technology, and CO_2 laser design. This thesis thus provides a repository of design techniques for future designers of sealed CO_2 waveguide lasers.

Secondly, this thesis fills a need for quantitative analysis of gas chemistry in sealed RF-excited CO_2 waveguide lasers. Although the lifetime advantages of RF excitation have been widely advertised, little substantive work concerning laser gas chemistry has been published. None of the papers published by Laakmann, the only producer of sealed RF-excited CO_2 waveguide lasers to

report research results, is sufficiently detailed to allow independent verification. The RF discharge studies of Williams and Smith did not always duplicate the conditions in working lasers nor could they produce any data with respect to laser output power. Data concerning laser lifetime and gas chemistry in sealed RF-excited CO_2 waveguide lasers could only be inferred from studies of DC-excited conventional and waveguide CO_2 lasers. The research results outlined in this thesis, concerning CO_2 dissociation and the effects of hydrogen and water vapor on laser output power, provide a valuable first step in the provision of detailed data which have been lacking in the literature.

It is obvious that a considerable body of work remains to be completed in order to meet the original objective of producing a 1000 hour-lifetime hard-sealed laser. Future work must extend the study of laser gas chemistry and continue the development of the prototype hard-sealed lasers. The most immediate requirement is to test the effectiveness of water vapor and/or hydrogen-absorbing getter materials such as phosphorus pentoxide, cellulose, and palladium. If the results of existing tests can be duplicated, operating lifetimes in excess of 1000 hours should be attainable.

Other lifetime-limiting factors which should be investigated include oxygen absorption and optical damage. Significant oxygen losses were observed even during short-term discharge tests. No direct effect on CO_2 dissociation was observed and further measurements are necessary in order to establish a threshold for this effect. If possible the source of oxygen absorption should be removed from the laser. Otherwise the net rate of oxygen absorption could be lessened by reducing CO_2 dissociation levels. The use of distributed platinum films may be the most effective means of achieving that goal.

The gradual loss in laser output power over the period of the laser gas chemistry experiments, attributed to optical damage, has not been adequately studied. The composition of the deposits on the optics should be identified using surface analysis techniques. Deposition rates may also be reduced by modifying the gas flow patterns inside the laser to reduce discharge streaming onto the optics. The prototype hard-sealed lasers, having ventilation of the waveguide through gas exchange channels and baffles which reduce the flow of gas around the ends of the waveguide, incorporate this design.

Through the development of a laser processing facility and the study of laser gas chemistry, this thesis has provided the necessary framework for the future development of hard-sealed long-life CO_2 waveguide lasers at the University of Alberta. The remaining challenge will be to integrate lifetime work with the results of high-power waveguide laser development.

REFERENCES

1 R. L. Abrams and W. B. Bridges, "Characteristics of Sealed-Off Waveguide CO_2 Lasers", *IEEE J. Quantum Electron.*, vol. QE-9, no. 9, pp. 940-946, 1973.

2 U. Hochuli, "Study of the CO_2 Waveguide Laser Life Problem", NASA Rep. NSG 5042, 1976.

3 L. M. Laughman, "Long-term operation of a sealed waveguide CO_2 laser", *Rev. Sci. Instrum.*, vol. 47, no. 11, pp. 1411-1413, 1976.

4 U. E. Hochuli and T. P. Sciacca, "Cold Cathodes for Sealed-Off CO_2 Lasers", *IEEE J. Quantum Electron.*, vol. QE-10, no. 2, pp. 239-244, 1974.

5 J. L. Lachambre, J. Macfarlane, G. Otis, and P. Lavigne, "A Transversely RF-Excited CO_2 Waveguide Laser", DREV Rep. M-2446/78, 1978.

6 K. D. Laakmann, "Transverse RF Excitation for Waveguide Lasers", *Proceedings of the International Conference on Lasers*, pp. 741-743, 1978, Orlando, Fla.

7 D. He and D. R. Hall, "A 30-W radio frequency excited waveguide CO_2 laser", *Appl. Phys. Lett.*, vol. 43, pp. 726-728, 1983.

8 K. D. Laakmann, P. Laakmann, " The coming of age of waveguide lasers", *SPIE*, vol. 247, pp. 74-78, 1980.

9 A. L. S. Smith and J. M. Austin, "Dissociation mechanism in pulsed and continuous CO_2 lasers", *J. Phys. D:Appl. Phys.*, vol. 7, pp. 314-322, 1974.

10 R. G. Buser and J. J. Sullivan, "Initial Processes in CO_2 Glow Discharges", *J. Appl. Phys.*, vol. 41, no. 2, pp. 472-479, 1970.

11 R. R. Reeves, P. Harteck, B. A. Thompson, and R. W. Waldron, "Photochemical Equilibrium Studies of Carbon Dioxide and Their Significance for the Venus Atmosphere", *J. Phys. Chem.*, vol. 70, no. 5, pp. 1637-1640, 1966.

12 W. J. Witteman, "High-Output Powers and Long Lifetimes of Sealed-Off CO_2 Lasers", *Appl. Phys. Lett.*, vol. 11, no. 11, pp. 337-338, 1967.

13 W. J. Witteman and H. J. Werner, " The Effect of Water Vapour and Hydrogen on the Gas Composition of a Sealed-Off CO_2 Laser", *Phys. Lett.*, vol. 26A, no. 10, pp. 454-455, 1968.

[14] A. L. S. Smith, "The Effect of Gas Flow on the Composition and Power Output of a CO_2 -He-N_2 Laser", *Phys. Lett.*, vol 27A, no. 7, pp. 432-433, 1968.

[15] A. L. S. Smith and P. G. Browne, "Catalysis in sealed CO_2 lasers", *J. Phys. D:Appl. Phys.*, vol. 7, pp. 1652-1659, 1974.

[16] F. M. Taylor, A. Lombardo, and W. C. Eppers, "Effect of a Heated Platinum Wire on a Sealed CO_2 Laser System", *Appl. Phys. Lett.*, vol. 11, no. 6, pp. 180-182, 1967.

[17] P. G. Browne and A. L. S. Smith, "Long-lived CO_2 lasers with distributed heterogeneous catalysis", *J. Phys. D:Appl. Phys.*, vol. 7, pp. 2464-2470, 1974.

[18] A. L. S. Smith, H. Shields, and A. E. Webb, "Cathode Materials for Sealed CO_2 Waveguide Lasers", *IEEE J. Quantum Electron.*, vol. QE-19, no. 5, pp. 815-820, 1983.

[19] I. E. Ross, J. Pithie, and J.G. Freeman, "Development of sealed CO_2 waveguide lasers", *SPIE*, vol. 236, pp. 329-334, 1980.

[20] K. D. Laakmann, US Patent No. 4,169,251 (assigned to Hughes Aircraft Co.), Sept. 25, 1979.

[21] G. Francis, *Ionization Phenomena in Gases*, Butterworths, London, pp. 81-172, 1960.

[22] G. C. R. Williams and A. L. S. Smith, "Plasma chemistry of RF discharges in CO_2 laser gas mixtures", *J. Phys. D:Appl. Phys.*, vol. 18, pp. 335-346, 1985.

[23] K. D. Laakmann, "Problems and status of reliability in rf-excited waveguide lasers", *SPIE*, vol. 328, pp. 2-6, 1982.

[24] T. F. Deutsch and F. A. Horrigan, "Life and Parameter Studies on Sealed CO_2 Lasers", *IEEE J. Quantum Electron.*, vol. QE-4, no. 11, pp. 972-975, 1968.

[25] P. K. Cheo and H. G. Cooper, "Gain characteristics of CO_2 laser amplifiers at 10.6 microns", *IEEE J. Quantum Electron.*, vol. QE-3, pp. 79-84, 1967.

[26] P. K. Cheo, "Relaxation of CO_2 Laser Levels by Collisions with Foreign Gases", *IEEE J. Quantum Electron.*, vol. QE-4, no. 10, pp. 587-593, 1968.

[27] P. Pace and J. Cruickshank, "Long-term operation of a sealed waveguide CO_2 laser", *Rev. Sci. Instrum.*, vol. 52, no. 10, pp. 1493-1496, 1981.

[28] P. Laakmann and K. D. Laakmann, "Sealed-Off RF Excited CO_2 Lasers and Method of Manufacturing Such Lasers", US Patent No. 4,393,506, Jul. 12, 1983.

[29] R. L. Sinclair, "Radio Frequency Excited CO_2 Gas Waveguide Lasers", M. Sc. Thesis, University of Alberta, Fall 1983.

[30] D. He and D. R. Hall, "Longitudinal voltage distribution in transverse rf discharge waveguide lasers", *J. Appl. Phys.*, vol. 54, no. 8, pp. 4367-4373, 1983.

[31] G. A. Griffith, "Improved discharge uniformity for transverse radio frequency waveguide CO_2 lasers", *SPIE*, vol. 335, pp. 69-71, 1982.

[32] P. C. Condor, R. M. Jenkins, V. G. Roper, E. W. Parcell, J. R. Redding, and T. W. Spencer, "A Compact Rugged CO_2 Waveguide Laser" in *Quantum Electronics and Electro-Optics*, P. L. Knight (ed.), J. Wiley, London, pp. 79-82, 1983.

[33] P. C. Condor, J. R. Redding, R. M. Jenkins, and T. W. Spencer, "Novel Techniques for CO_2 Waveguide Laser Construction", *CLEO*, Anaheim, June 1984, paper TuBb.

[34] R. A. Hill, C. F. Brown, G. A. Griffith, L. V. Sutter, F. A. Dolezal, R. D. Washburn, and E. R. Peressini, "Development of a flyable CO_2 laser beacon", *SPIE*, vol. 227, pp. 12-15, 1980.

[35] A. H. Beck, *Handbook of Vacuum Physics*, vol. 3, Pergamon, London, pp. 33-40, 1964.

[36] J. F. O'Hanlon, *A User's Guide to Vacuum Technology*, J. Wiley, New York, p. 132, 1980.

[37] A. Schram, "La desorption sous vide", *Le Vide*, vol. 103, p. 55, 1963.

[38] J. R. Young, "Outgassing Characteristics of Stainless Steel and Aluminum with Different Surface Treatments", *J. Vac. Sci. Technol.*, vol. 6, p. 398, 1969.

[39] R. Nuvalone, "Technology of low-pressure systems - establishment of optimum conditions to obtain low degassing rates on 316L stainless steel by heat treatments", *J. Vac. Sci. Technol.*, vol. 14, p. 1210, 1977.

[40] R. Calder and G. Lewin, "Reduction of Stainless Steel Outgassing in Ultrahigh Vacuum", *Brit. J. Appl. Phys.*, vol. 18, p. 1459, 1967.

[41] B. H. Colwell, "Outgassing rates of refractory and electrical insulating materials used in high vacuum furnaces", *Vacuum*, vol. 20, p. 481, 1970.

[42] S. Dushman, *Scientific Foundations of Vacuum Theory*, J. Wiley, New York, 1962.

[43] S. M. Neale and W. A. Stringfellow, "The Primary Sorption of Water by Cotton", *Trans. Faraday Soc.*, vol. 37, pp. 525-532, 1941.

[44] Murray Paulson is currently a member of the Medical Laser Lab, Department of Electrical Engineering, University of Alberta.

[45] E. S. Gasilevich, V. A. Ivanov, E. N. Lotkova, V. N. Ochkin, N. N. Sobolev, and N. G. Yaroslavskii, "Carbon Dioxide Dissociation in a CO_2 Laser", *Soviet Phys. - Tech. Phys.*, vol. 41, no. 1, pp. 86-91, 1969.

[46] R. J. Carbone, "Long-Term Operation of a Sealed CO_2 Laser", *IEEE J. Quantum Electron.*, vol. QE-3, no. 9, pp. 373-375, 1967.

[47] P. D. Tannen, P. Bletzinger, and A. Garscadden, "Species Composition in the CO_2 Discharge Laser", *IEEE J. Quantum Electron.* , vol. QE-10, no. 1, pp. 6-11, 1974.

[48] N. Karube and E. Yamaka, "Mass spectroscopic studies of a sealed CO_2 laser", *J. Appl. Phys.*, vol. 41, no. 5, pp. 2031-2042, 1970.

[49] D. S. Stark and M. R. Harris, "Platinum-catalyzed recombination of CO and O_2 in sealed CO_2 TEA laser gases", *J. Phys. E:Sci. Instrum.*, vol. 11, pp 316-319, 1978.

[50] H. J. Schotzau, F. Conti, R. Gindrat, and F. K. Kneubuhl, "Mass Spectroscopy of the Plasma of CW and TEA CO_2 Laser Discarges", *Phys. Lett.*, vol. 48A, no. 3, pp. 205-206, 1974.

[51] S. M. Fry, "Waveguide CO_2 laser lifetest", *CLEO*, 1980, paper TUKK5.

[52] H. E. Evans and P. P. Jennings, "Mass-Spectrometric Study of the Species present in R.F. Discharges in CO_2, CO, and O_2", *Trans. Faraday Soc.*, vol. 61, pp. 2153-2160, 1965.

[53] D. H. Biswas and U. K. Chatterjee, "Gas-Chromatographic Studies of the Products in a Sealed TE CO_2 Laser Discharge", *IEEE J. Quantum Electron.*, vol. QE-17, no. 9, pp. 1964-1966, 1981.

[54] C. Willis and J. G. Purdon, "Catalytic control of the gas chemistry of sealed TEA CO_2 lasers", *J. Appl. Phys.*, vol. 50, no. 4, pp. 2539-2543, 1979.

[55] P. Capezzuto, F. Cramarossa, Riccardo d'Agostino, and E. Molinari, "Contribution of Vibrational Excitation to the Rate of Carbon Dioxide Dissociation in Electrical Discharges", *J. Phys. Chem.*, vol. 80, no. 8, pp. 882-888, 1976.

[56] J. J. Sullivan and R. G. Buser, "Mass Spectroscopic Sampling of Glow Discharges", *J. Vac. Sci. Technol.*, vol. 6, pp. 103-108, 1969.

[57] R. A. A. Kubiak, W. Y. Leong, R. M. King, and E. H. C. Parker, "On baking a cryopumped UHV system", *J. Vac. Sci. Technol. A*, vol. 1, no. 4, pp. 1872-1873, 1983.

[58] M. J. Drinkwine and D. Lichtman, *Partial Pressure Analyzers and Analysis*, American Vacuum Society Monograph Series.

[59] Technical Reference Manual, SM100D Residual Gas Analyzer, Spectrum Scientific Ltd., Congleton, England, section 6.14, 1983.

[60] The cracking pattern for Xe is dominated by five singely ionized isotopic peaks at masses 129, 131, 132, 134, and 136 and five doubly ionized isotopic peaks at masses 64.5, 65.5, 66, 67, and 68. As the RGA had an upper mass limit of 100, the the largest doubly ionized peak at mass 64.5 was considered to be the principal peak.

[61] R. Dobrozemsky, "Experience with a Computer Program for Residual Gas Analyzers", *J. Vac. Sci. Technol.* , vol. 9, p. 220, 1972.

[62] Matheson Primary Standards are calibration gas mixtures precisely blended by weighing the gas components on a high load, high sensitivity analytical balance. All weights used on this balance are NBS traceable. Certification accuracy is 0.02% absolute or 1% of the component value, which ever is larger.

[63] Y. E. Strausser, "The effect of surface treatment on the outgassing rates of 304 stainless steel", *Proc. 4th Intl. Vac. Cong.*, part 2, pp. 469-472, 1968.

[64] R. L. Sinclair and J. Tulip, "Radio frequency excited CO_2 waveguide lasers", *Rev. Sci. Instrum.*, vol. 55, no. 10, pp. 1539-41, 1984.

[65] A. N. Vargin, V. V. Gogokhiya, V. K. Konyakhov, and L. M. Pasynkova, "Rates of resonant vibrational exchange between the CO_2 molecule and N_2 and CO molecules", *Sov. J. Quantum Elec.*, vol. 6, pp. 119-121, 1976.

[66] Water vapor concentrations are estimates obtained by measuring the ratio of the principal peak at mass 18 to that of CO_2 at mass 44.

[67] P. Bletzinger, D. A. LaBorde, W. F. Bailey, W. H. Long, P. Tannen, and A. Garscadden, "Influence of Contaminants on the CO_2 Electric-Discharge Laser", *IEEE J. Quantum Elec.*, vol. QE-11, no. 7, pp. 317-323, 1975.

[68] P. Vidaud and D. R. Hall, "Effect of xenon on the electron temperature of rf discharge CO_2 laser gas mixtures", *J. Appl. Phys.*, vol. 57, no. 5, pp. 1757-1758, 1985.

[69] A. E. Belyanko, N. I. Lipatov, P. P. Pashinin, and Yu. N. Polivanov, "Waveguide CO_2 laser with 7.5 W output power", *Sov. J. Quantum Elec.*, vol. 14, no. 1, pp. 123-126, 1984.